EXCITED QCD 2018
Kopaonik, Serbia
11-15 March 2018

Recent tests of QCD with the ATLAS detector

Giuseppe Callea on behalf of the ATLAS collaboration

Istituto Nazionale di Fisica Nucleare

UNIVERSITÀ DELLA CALABRIA

14/03/2018

Outline

- Study of ordered hadron chains (***Phys. Rev. D 96 (2017) 092008***).

Physics with jets

- Softdrop jet substructure measurement (***arXiv:1711.08341***);
- Inclusive jet at 8 TeV (***JHEP 09 (2017) 020***);
- Inclusive jets and dijets at 13 TeV (***arXiv:1711.02692***).

Exclusive production

- Exclusive dilepton production at 7 TeV(***Phys. Lett. B 749 (2015) 242***);
- Exclusive $\mu^+\mu^-$ production at 13 TeV (***Phys. Lett. B 777 (2018) 303***);
- Exclusive W^+W^- cross section at 8 TeV ***(Phys. Rev. D 94 (2016) 032011***).

Ordered hadron chains

- Important source of information about early stages of hadron formation;
- Test of QCD string fragmentation model;
- 3D helical string model (**Phys.Rev. D89 (2014) 015002**) ⟶ Predicts excess of like-sign hadrons with small Q.

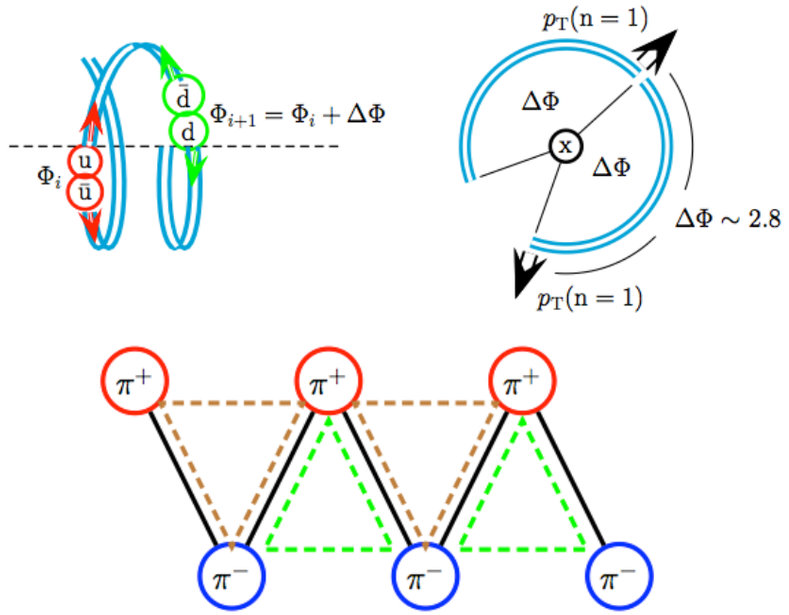

Chain of 3 charged hadrons from which the helix properties can be inferred.

- Each particle is paired with like-sign particle that minimizes Q;
- Each pair is supplemented with an opposite particle chosen to minimize the triplet mass.

Need to build a correlation function to discriminate the combinatorial background.

$$\Delta(Q) = \frac{1}{N_{ch}}[N(Q)^{OS} - N(Q)^{LS}]$$

Similar shape with $\Delta_{3h}\,(Q)$ at low Q values.

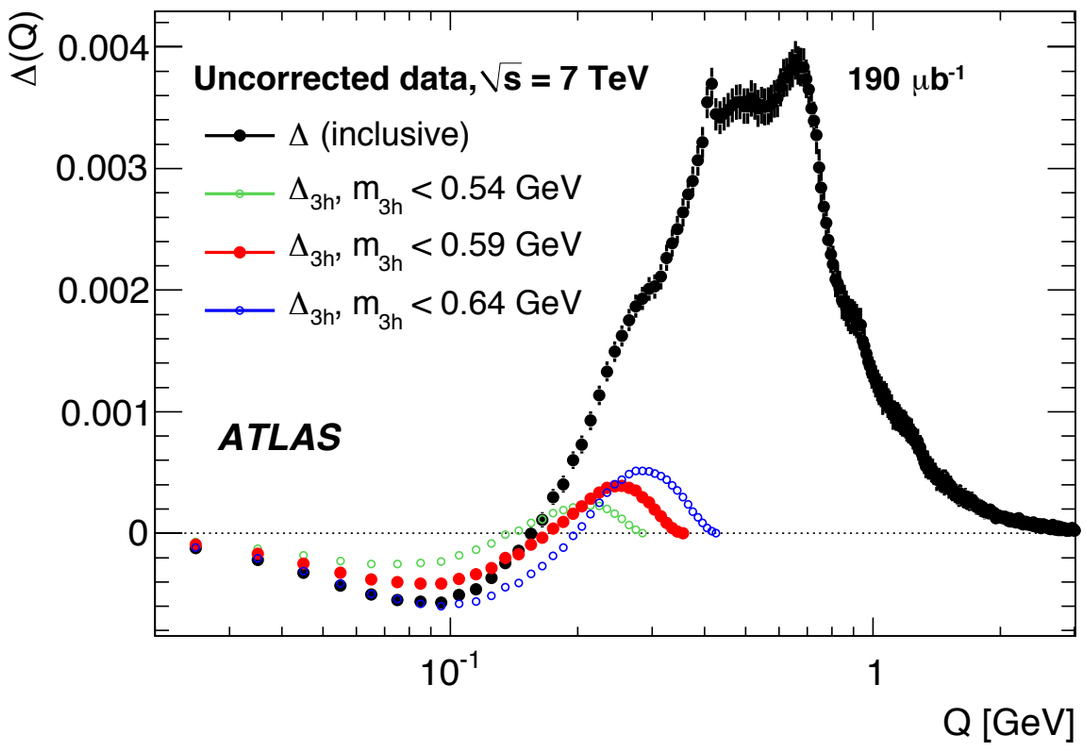

Ordered hadron chains

Enhanced like-sign production at low Q, traditionally attributed to Bose-Einstein effect.

$m_{3h}^{ch} = 591 \pm 2(stat) \pm 7(syst)$ MeV, in agreement with the predictions of helix fragmentation model ($m_3 = 570 \pm 20$ MeV).

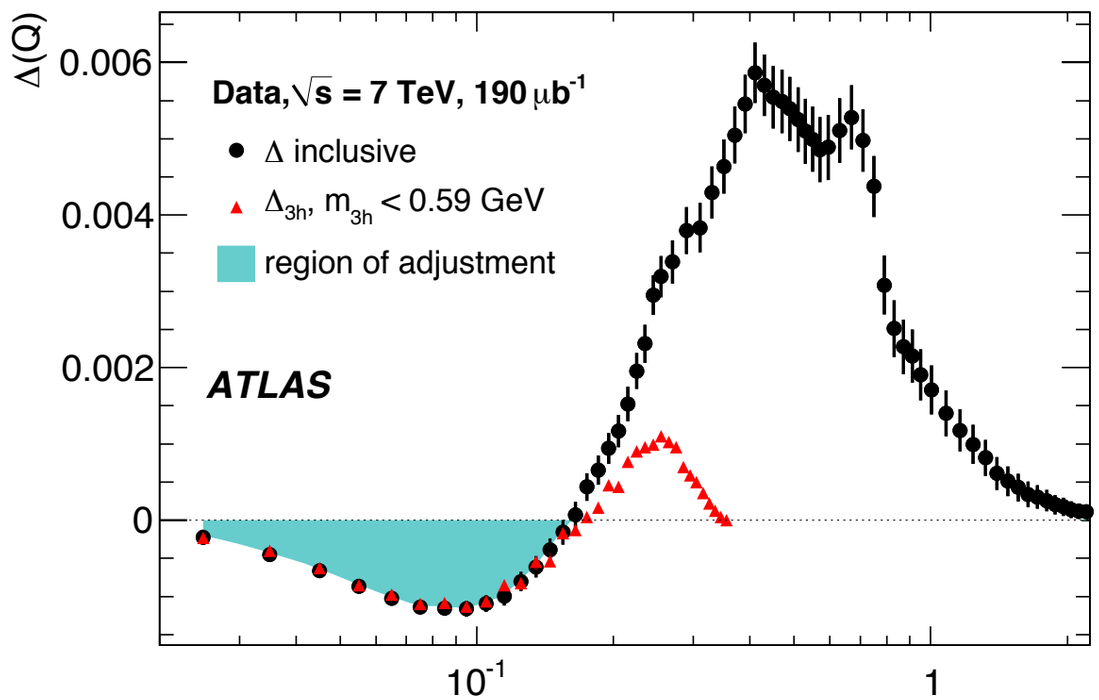

Dalitz plot coordinates:

$$X = \sqrt{3}\frac{T_0 - T_2}{\sum_{i=0}^{2} T_i} \qquad Y = \frac{3T_1}{\sum_{i=0}^{2} T_i} - 1$$

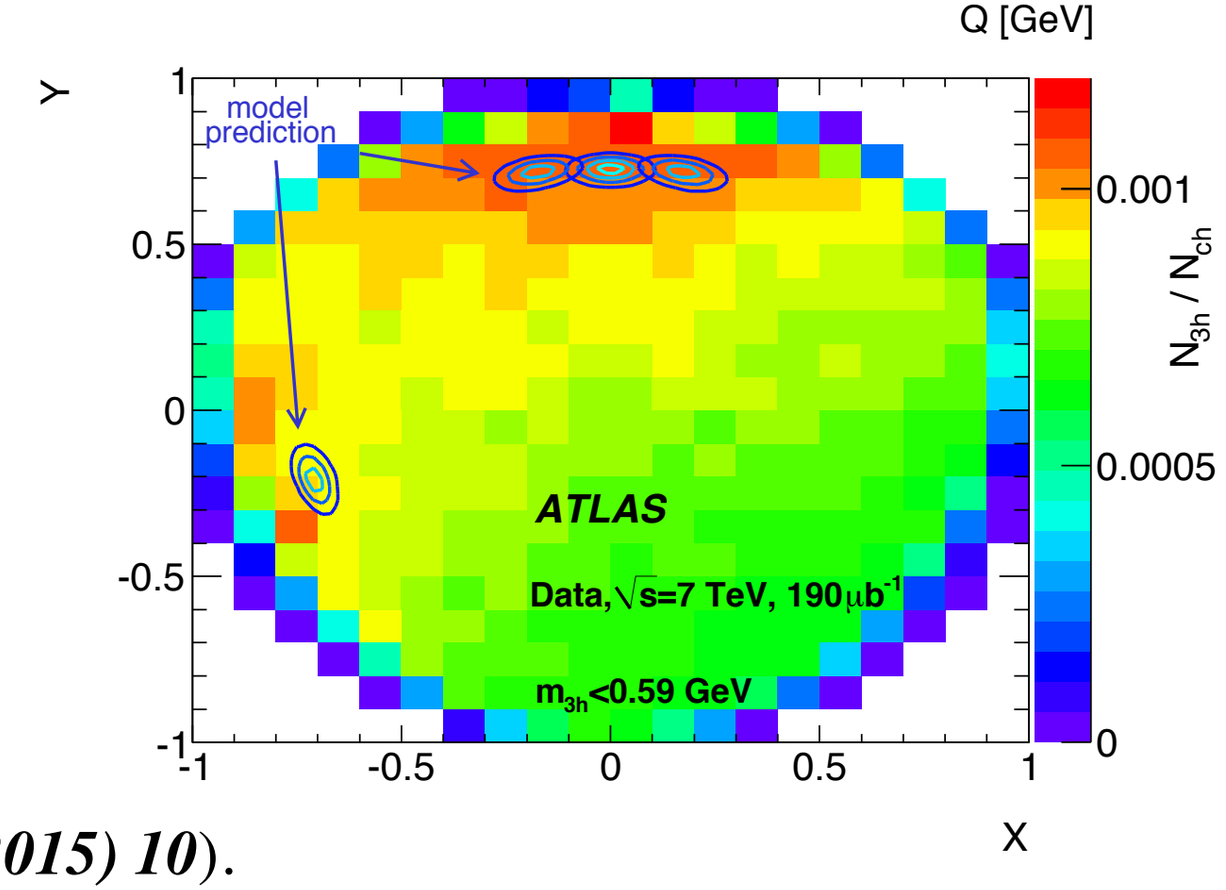

Data show a threshold effect in the production of adjacent hadron pairs, it coincides with preferred momentum difference between opposite-sign pairs in the selected chains.

Bose-Einstein correlations (***Eur. Phys. J C75 (2015) 10***).

Physics with jets

- Test of perturbative QCD predictions;
- Constraint on proton PDFs;
- Determination of the strong coupling constant (***Eur. Phys. J. 77 (2017) 872***);
- Description of background event kinematic for different searches for new physics.

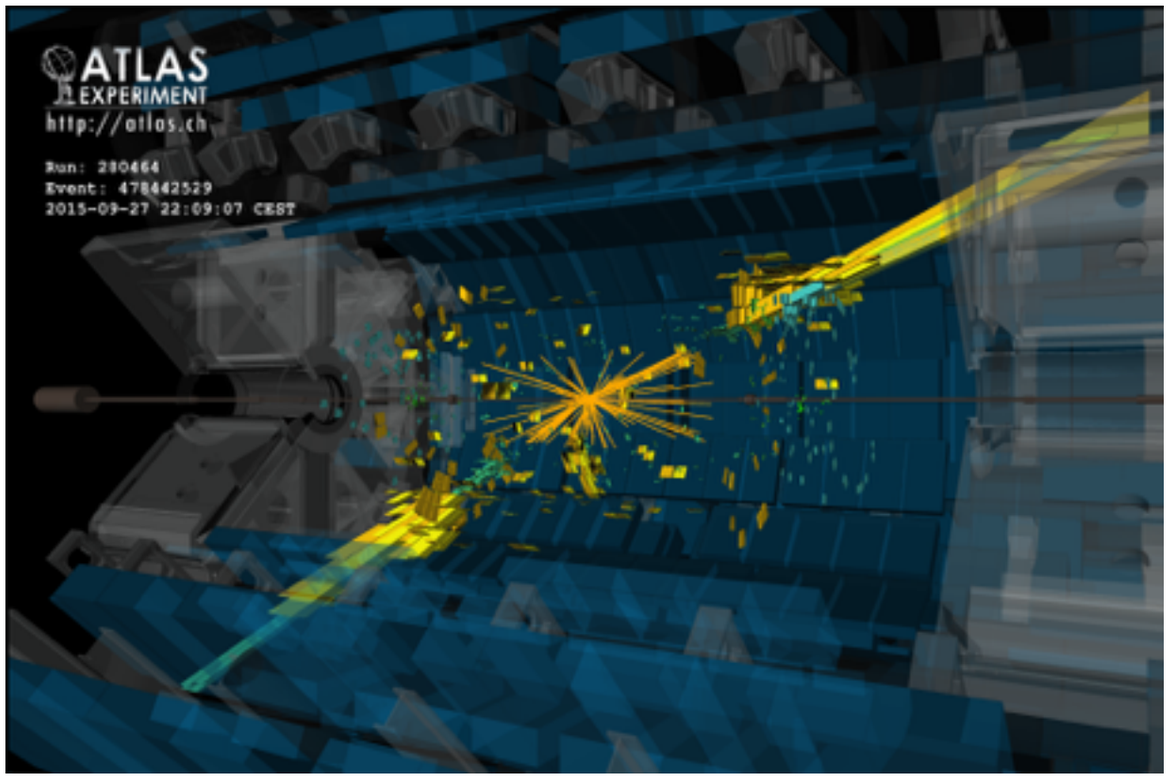

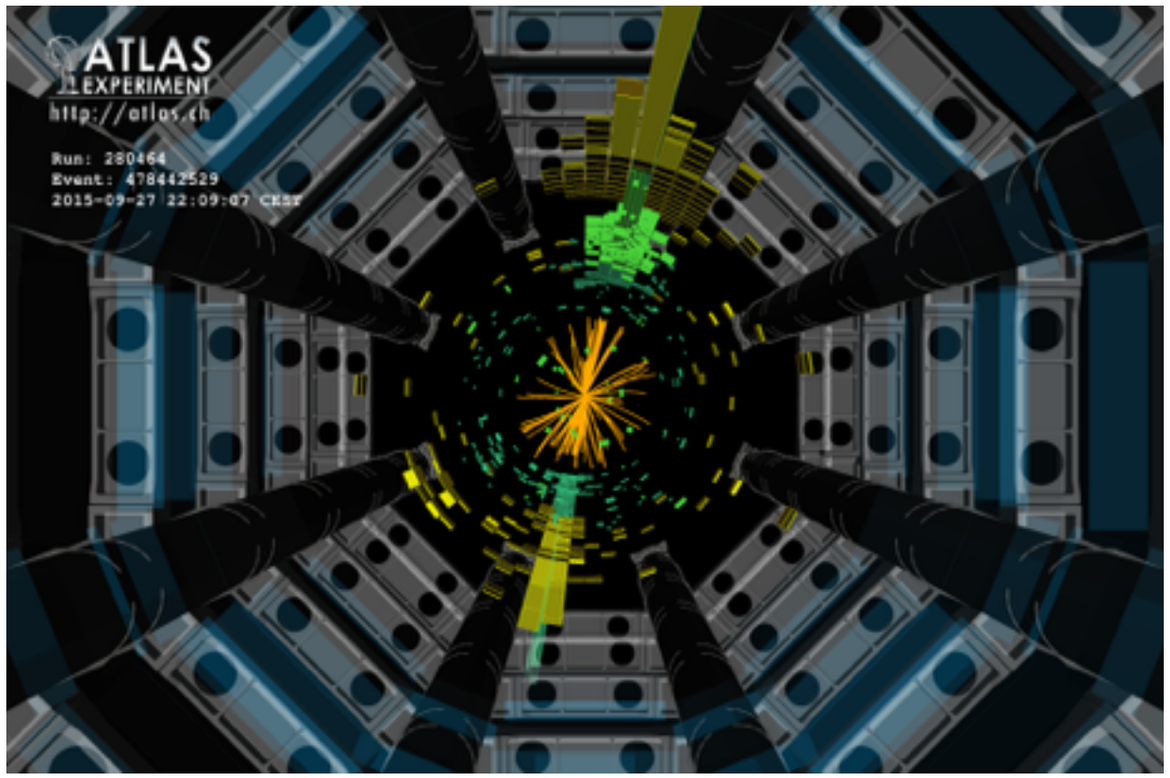

Soft-drop algorithm

- Jet grooming procedure to remove soft and wide angle radiation from a jet;
- Formally insensitive to non-global logarithms (***arXiv:1004.3483***);
- Take an anti-k_t jet and clusters its components using the Cambridge/Aachen algorithm.

Soft-drop condition:

$$\frac{min(\mathrm{p_{T,j_1}},\mathrm{p_{T,j_2}})}{\mathrm{p_{T,j_1}}+\mathrm{p_{T,j_2}}} > z_{cut}\left(\frac{\Delta R_{12}}{R}\right)^{\beta}$$

As β increases, the fraction of branches where the condition is satisfied increases, reducing the amount of radiation removed.

The mass of the resulting jet is called the soft-drop jet mass $m^{\mathrm{soft-drop}}$.

$\rho = \frac{m^{\mathrm{soft-drop}}}{p_{\mathrm{T}}^{\mathrm{ungroomed}}}$ weakly depends on p_{T} .

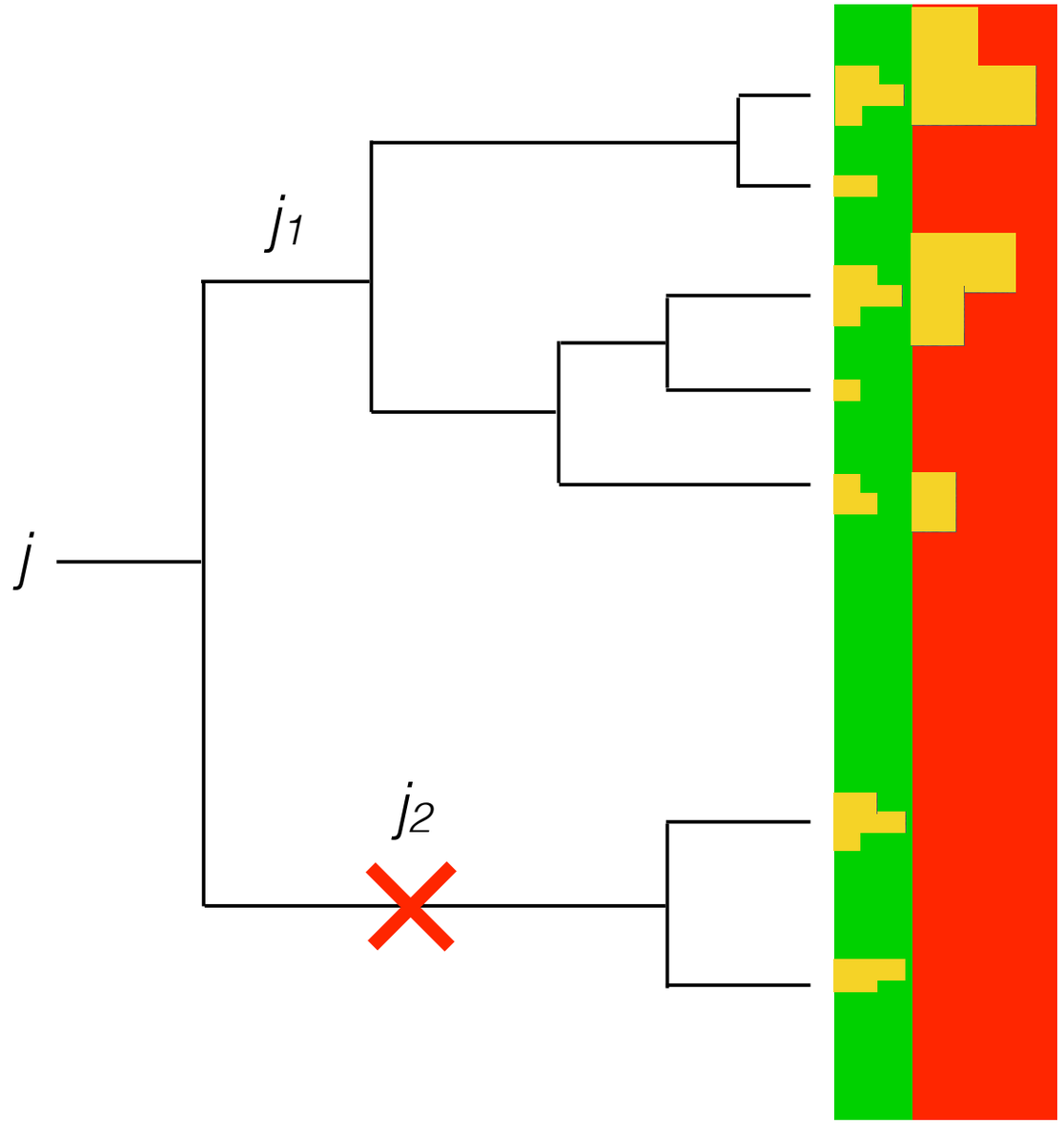

Soft-drop algorithm

Measured in dijet events: anti-k_t (0.8) jets, $p_{\mathrm{T}} > 600$ GeV, $|\eta| < 1.5$.
$p_{\mathrm{T},1}/p_{\mathrm{T},2} < 1.5$ to remove events with additional energetic jets.

$\beta \in (0, 1, 2)$, $Z_{\mathrm{cut}} = 0.1$

-3.7$< \log_{10}(\rho^2) <$ -1.7 **resummation region**

The measured and predicted shapes are in good agreement in the resummation region.
At low $\log_{10}(\rho^2)$ values, for large NP effects, NLO+NLL (which includes NP corrections) continue to agree with data within uncertainties.

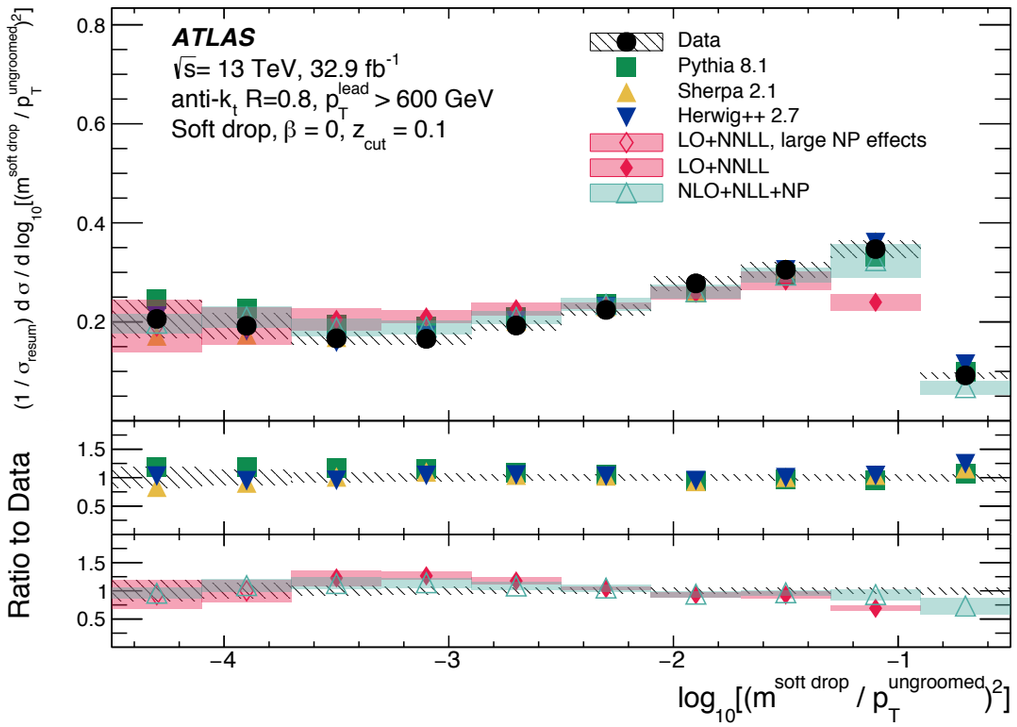

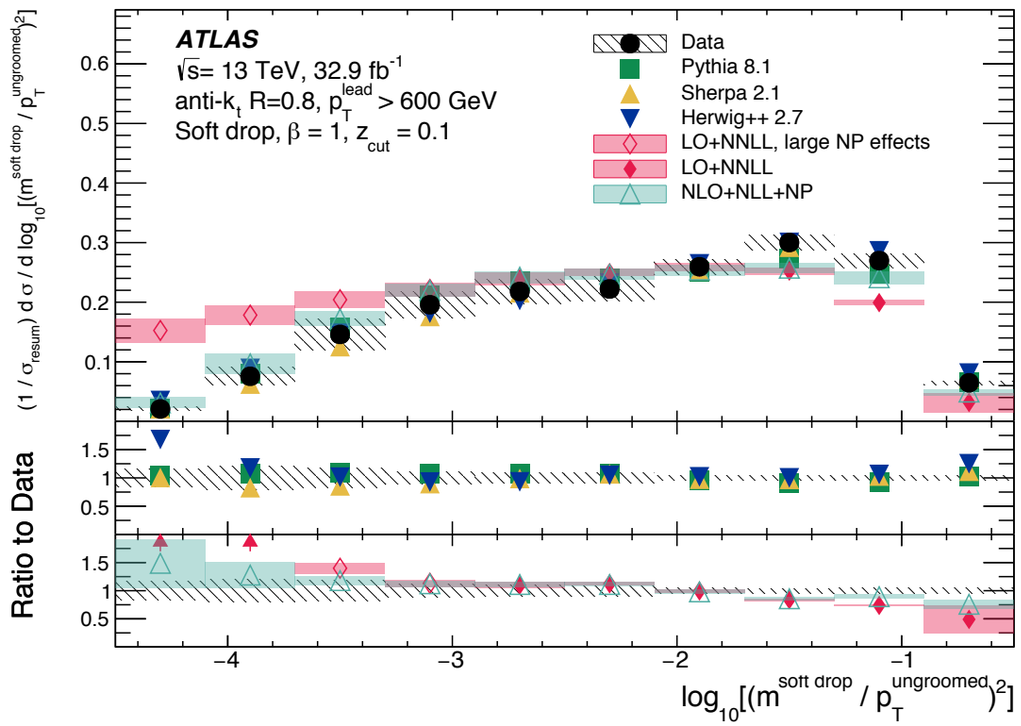

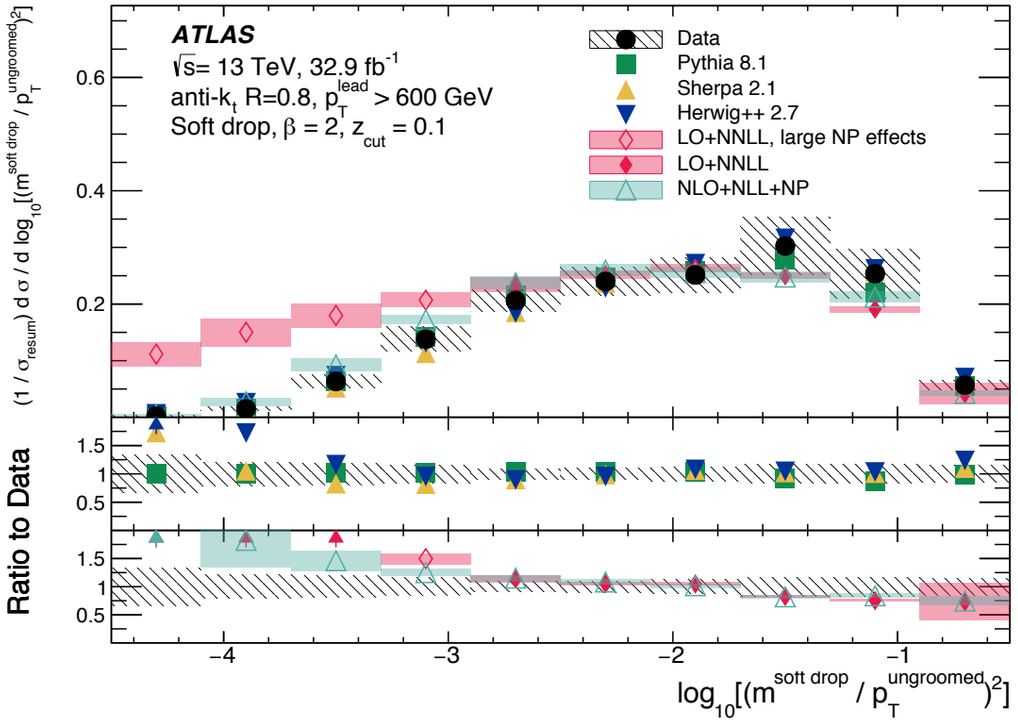

Inclusive Jet production

$\sqrt{s} = 8$ TeV $\qquad pp \to Jet + X \qquad$ $\sqrt{s} = 13$ TeV

- $P_T > 70$ GeV;
- $|y| < 3$;
- anti-kt jets with both R=0.4 and R=0.6;

- $P_T > 100$ GeV;
- $|y| < 3$;
- Only R=0.4 anti-kt jets;

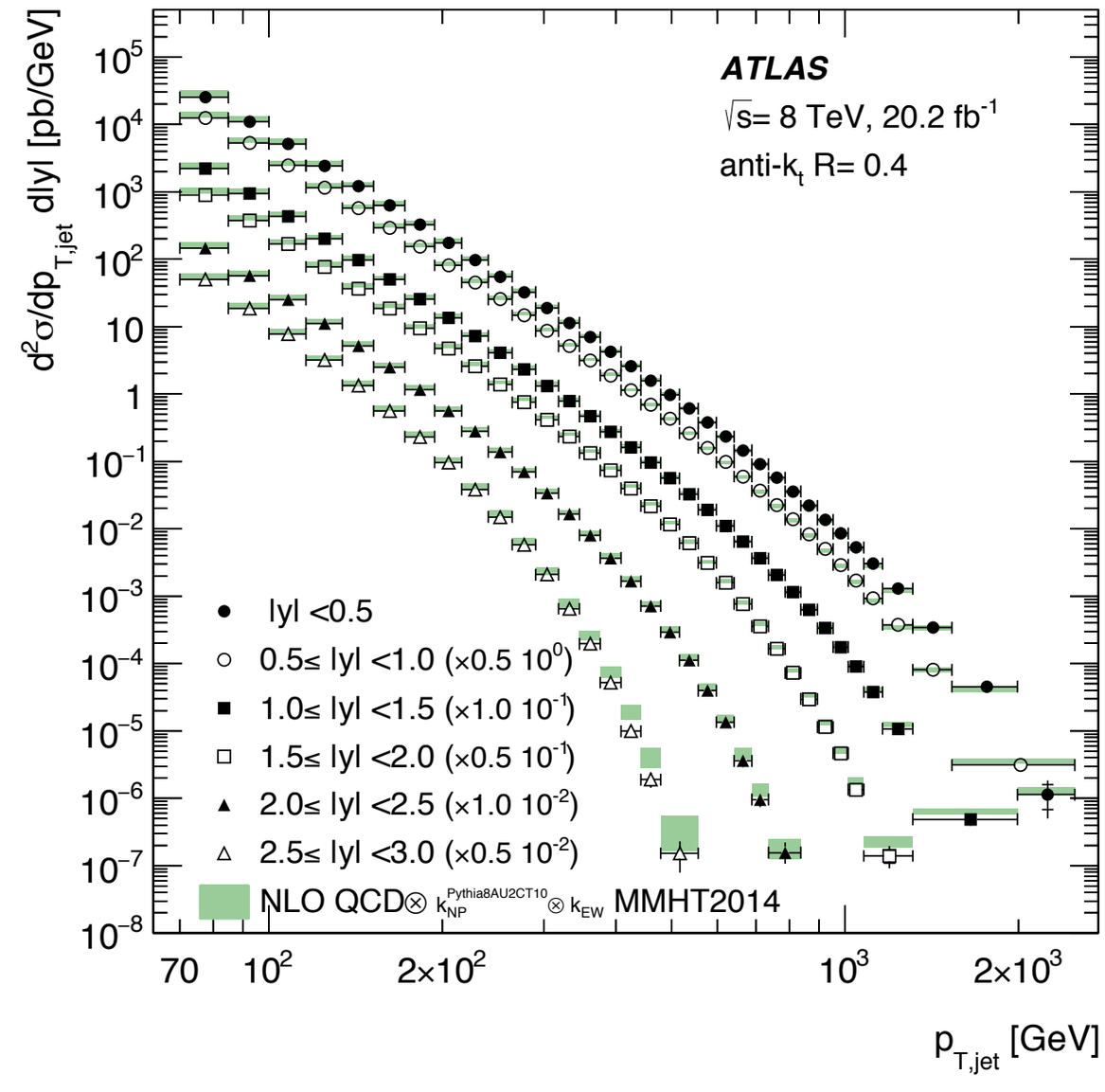

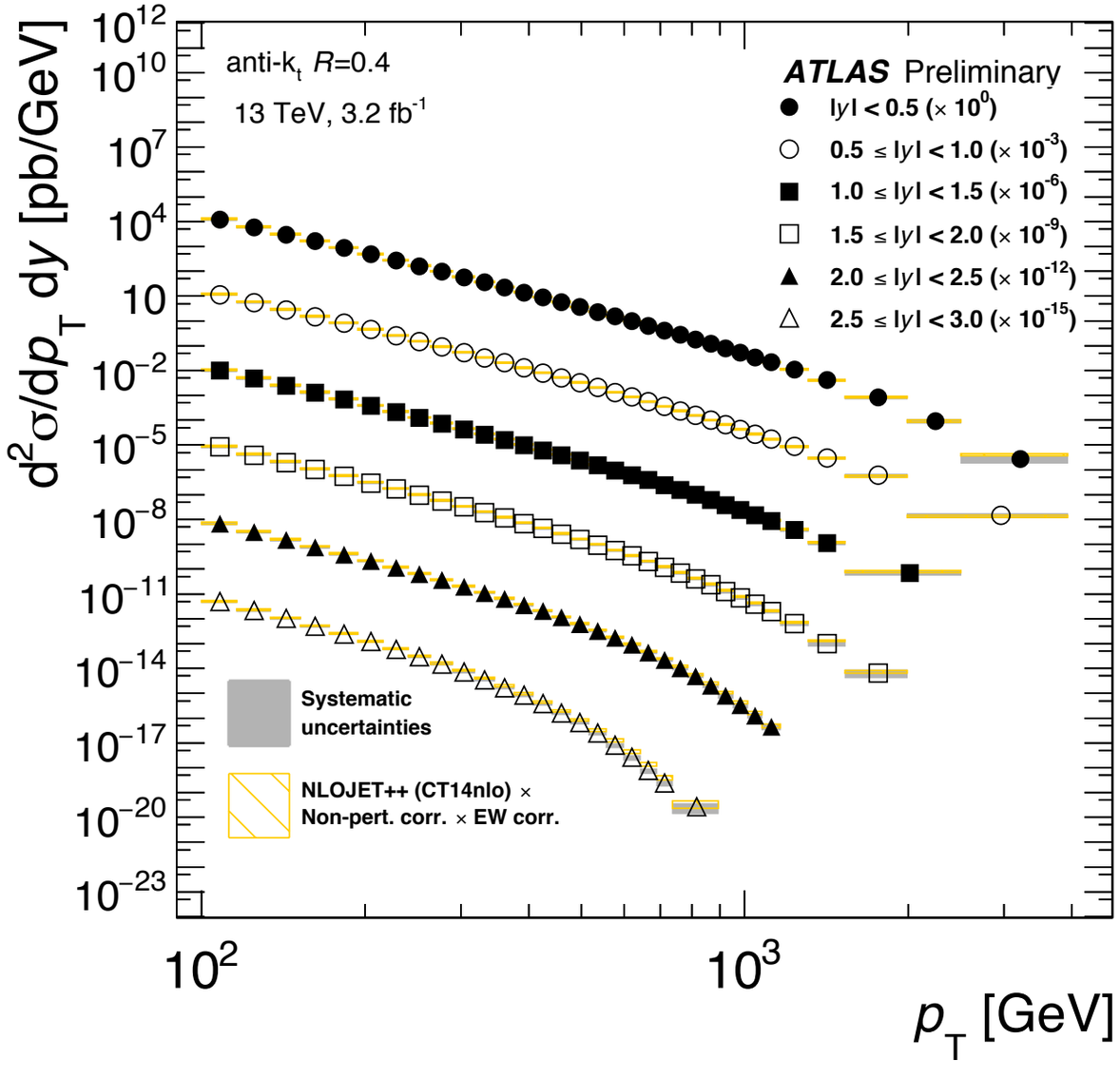

Inclusive Jet production

Quantitative comparison between data and theoretical prediction.

NLO QCD predictions (corrected for non-perturbative and EW effects) are typically above the data for $P_T \leq 100$ GeV.
Better agreement for higher P_T, except for $P_T > 1$ TeV where the NLO QCD predictions are higher (10-20%) than data.
Same behavior observed for different PDF sets.

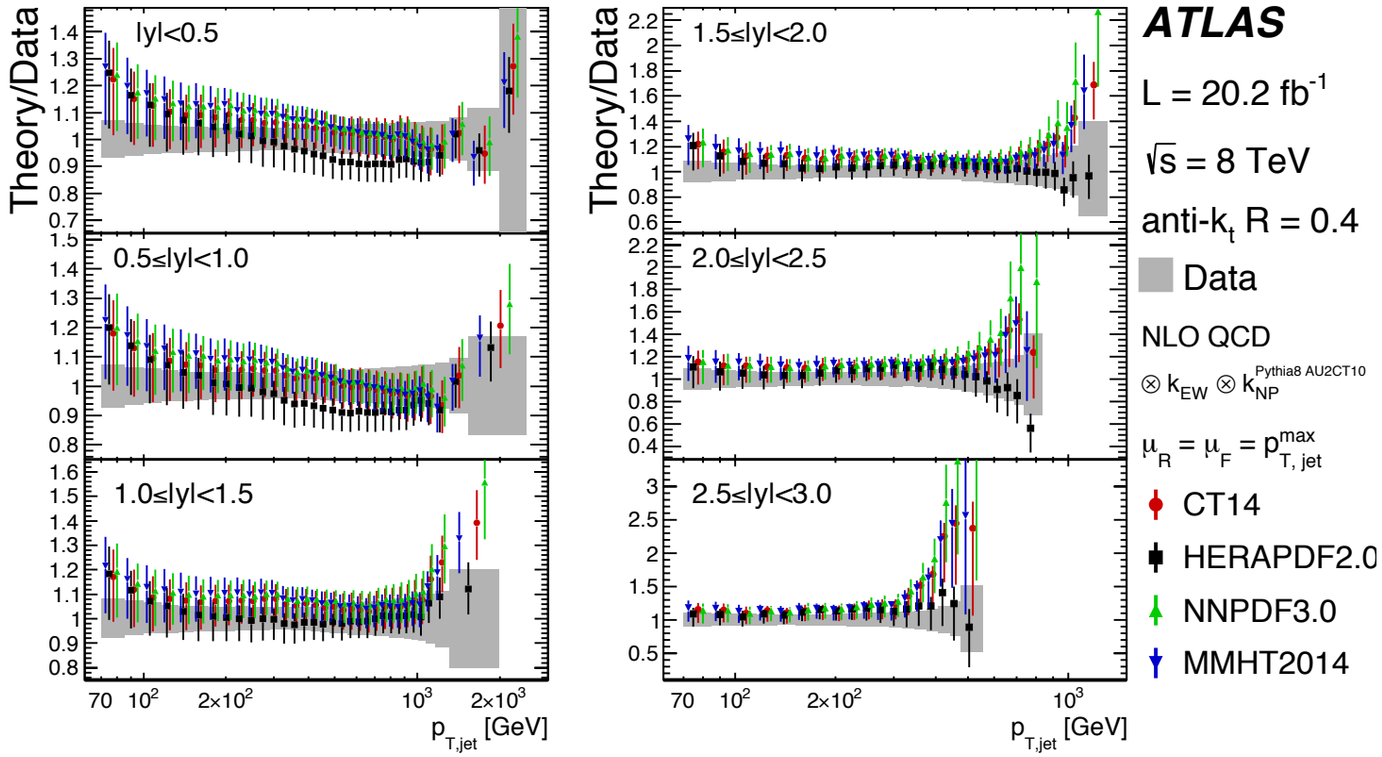

NNLO pQCD prediction based on:

- ***arXiv: 1611.01460***;
- ***arXiv: 1704.00923***;

are available at 13 TeV.

Two different scale choices P_T^{jet} and P_T^{max} (**backup slide**).
No significant deviations from data are observed, except at $|y| > 2.5$.

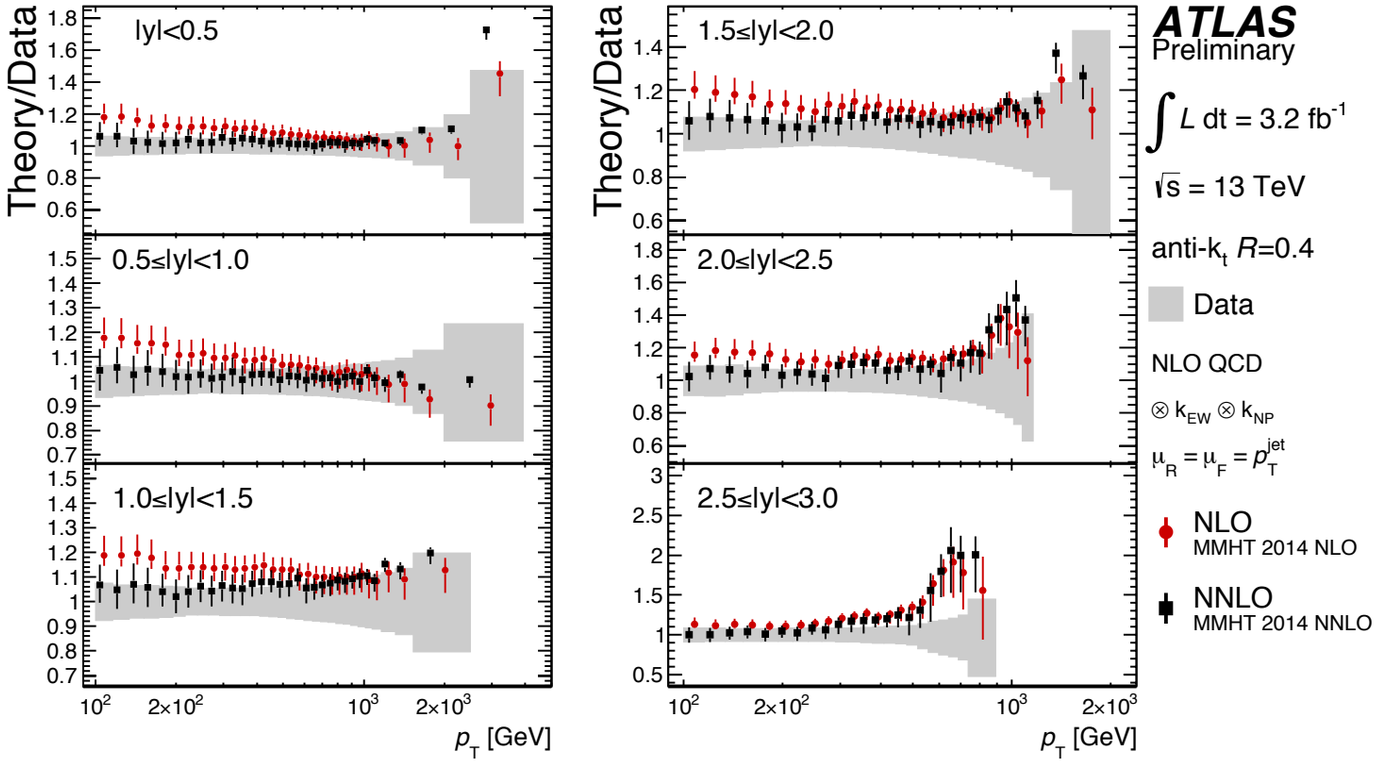

Dijet production at 13 TeV

- At least two jets with $P_T > 75$ GeV, within the interval $|y| < 3$;
- $H_{T,2} = P_{T1} + P_{T2}$ has to be higher than 200 GeV;

Double differential cross section is measured as a function of the invariant mass of the dijet system, m_{jj}, in $y^* = |y_1 - y_2|/2$ bins.

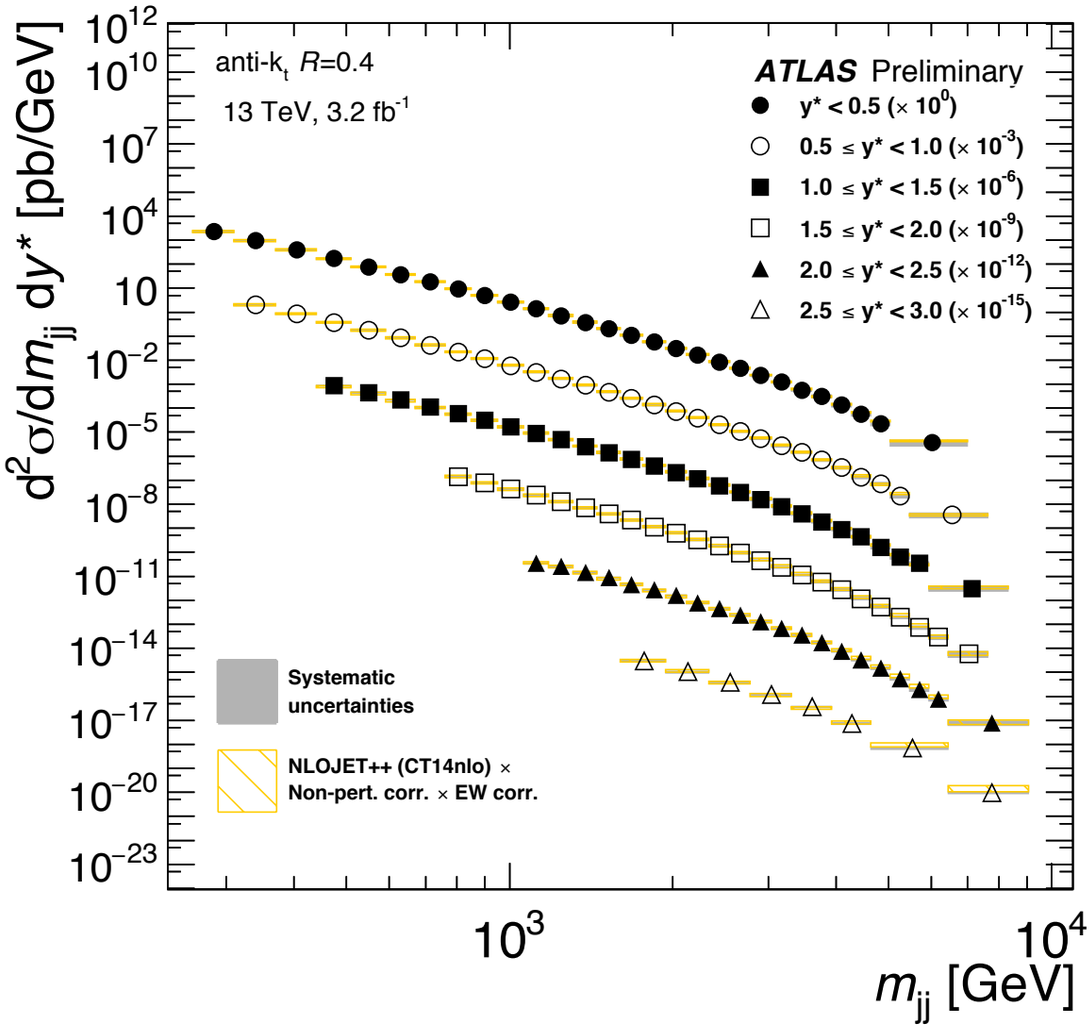

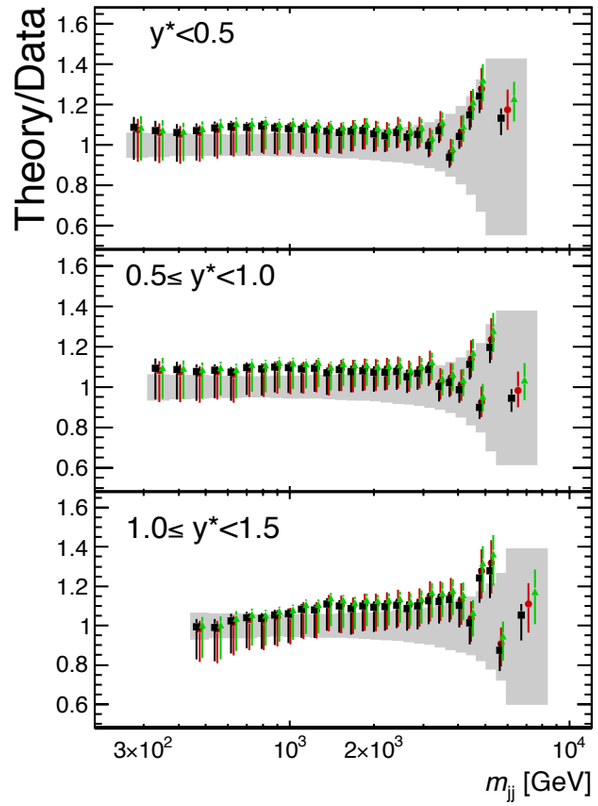

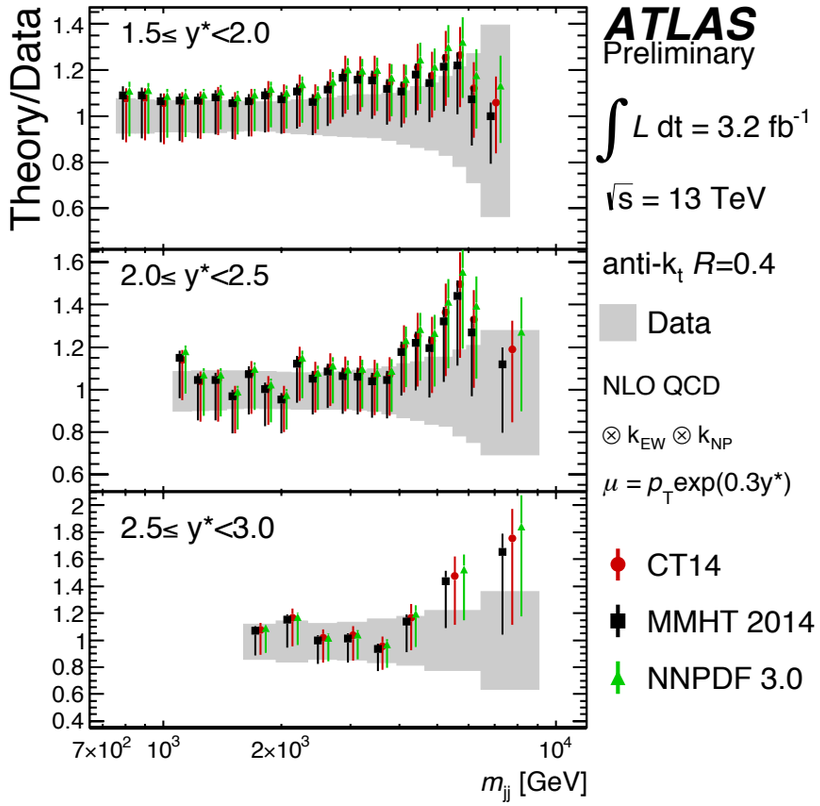

Fair agreement between data and NLO QCD predictions within the experimental uncertainties.

Exclusive production

- Induced interactions provide unique opportunity to study high-energy electroweak processes ($pp(\gamma\gamma) \to p + A + p$, A= $\ell^+\ell^-$, W^+W^-, H, etc.);
- No additional activity associated to the exclusive production vertex;
- Signal modeled following the Equivalent Photon Approximation (EPA);

→ colliding protons produce quasi-real photons with low virtuality $Q^2 < 0.1\,\text{GeV}$;

→ convolving the photon fluxes with the exclusive process cross section.

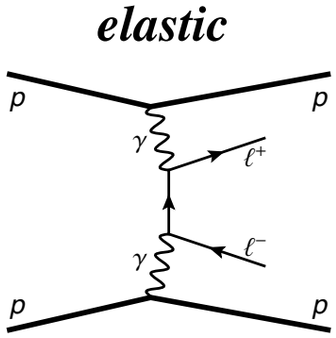

elastic

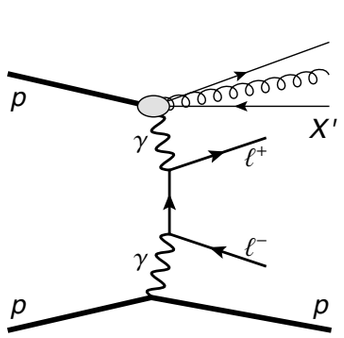

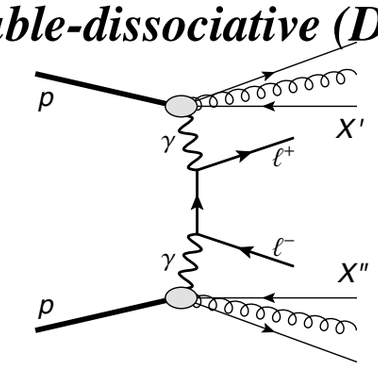

double-dissociative (DD)

single-dissociative (SD)

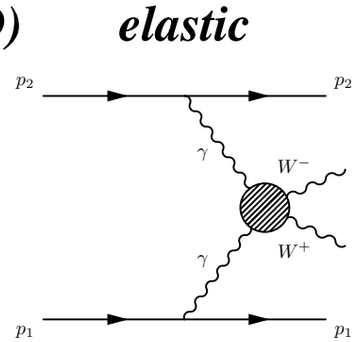

elastic

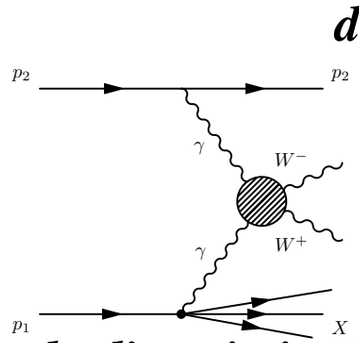

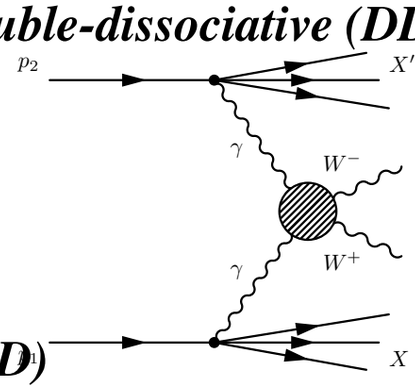

double-dissociative (DD)

single-dissociative (SD)

Single-dissociative ⟶ One proton fragments in the final state.

Double dissociative ⟶ Both protons fragment in the final state.

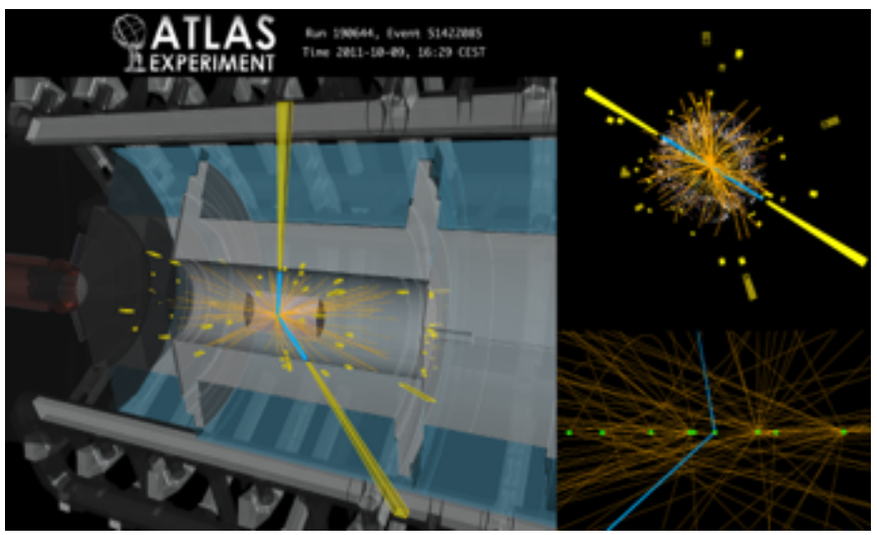

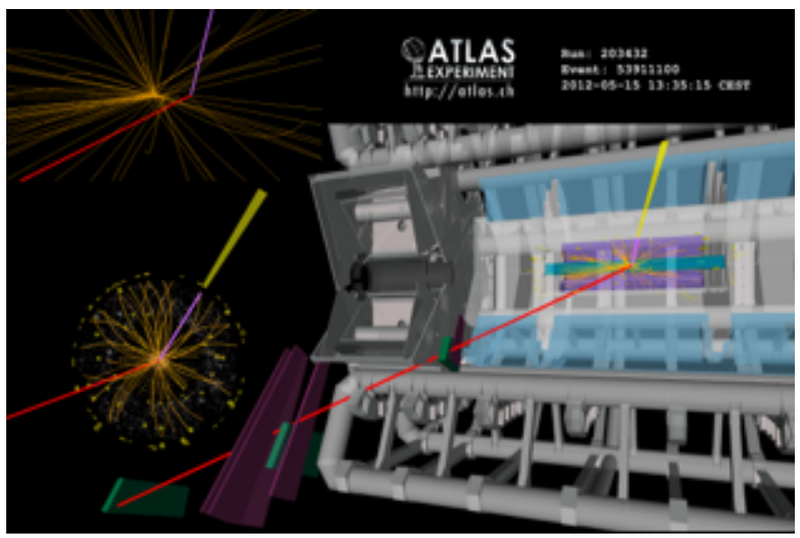

$\gamma\gamma \to \ell^+\ell^-$ *at 7 TeV*

- Direct access to the elastic photon distributions in proton;
- Non-negligible background to the Drell-Yan processes.

Exclusive event selection:

- Exactly 2 tracks, veto on additional tracks ($\mathrm{p_T} > 0.4$ GeV);
- 3 mm dilepton vertex longitudinal isolation;
- Remove events with $70\ \mathrm{GeV} < M_{\ell\ell} < 105\ \mathrm{GeV}$;
- ${\mathrm{p_T}}^{\ell\ell} < 1.5$ GeV to suppress dissociative background.

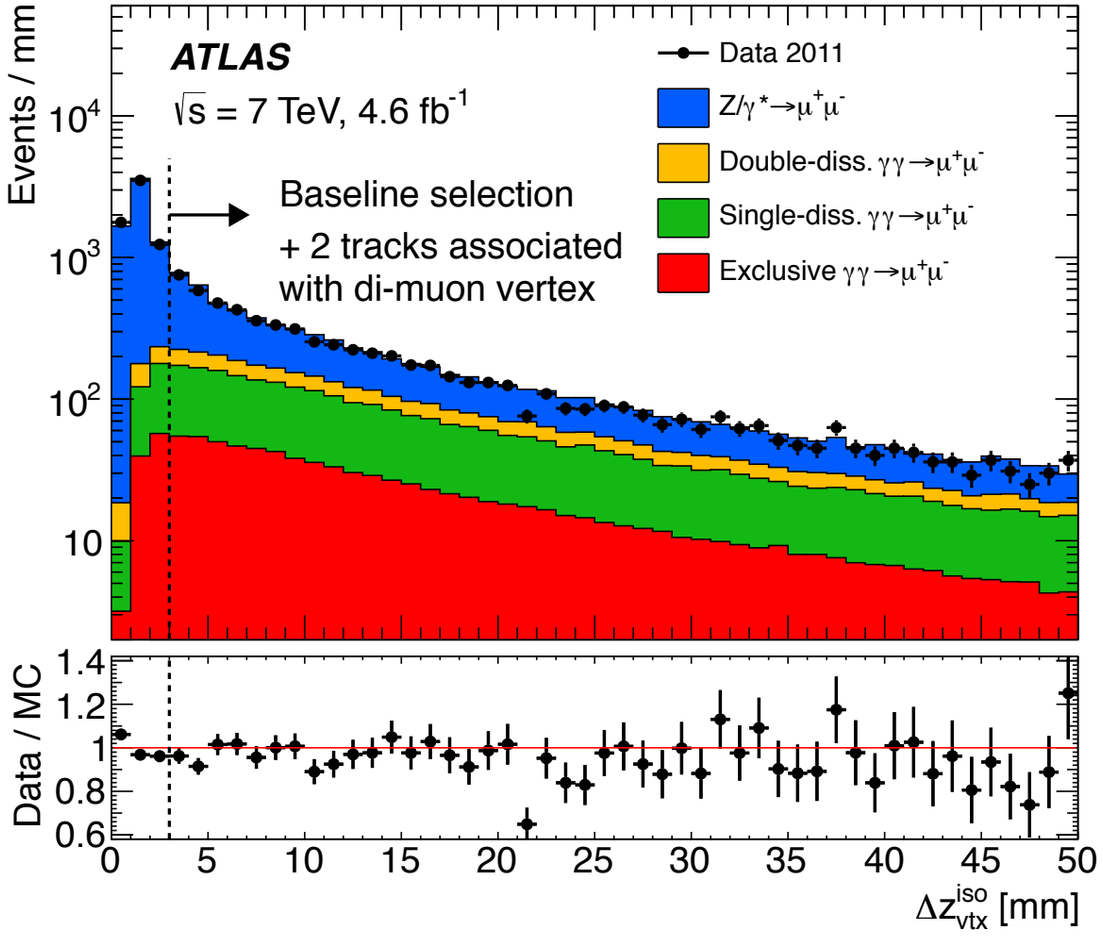

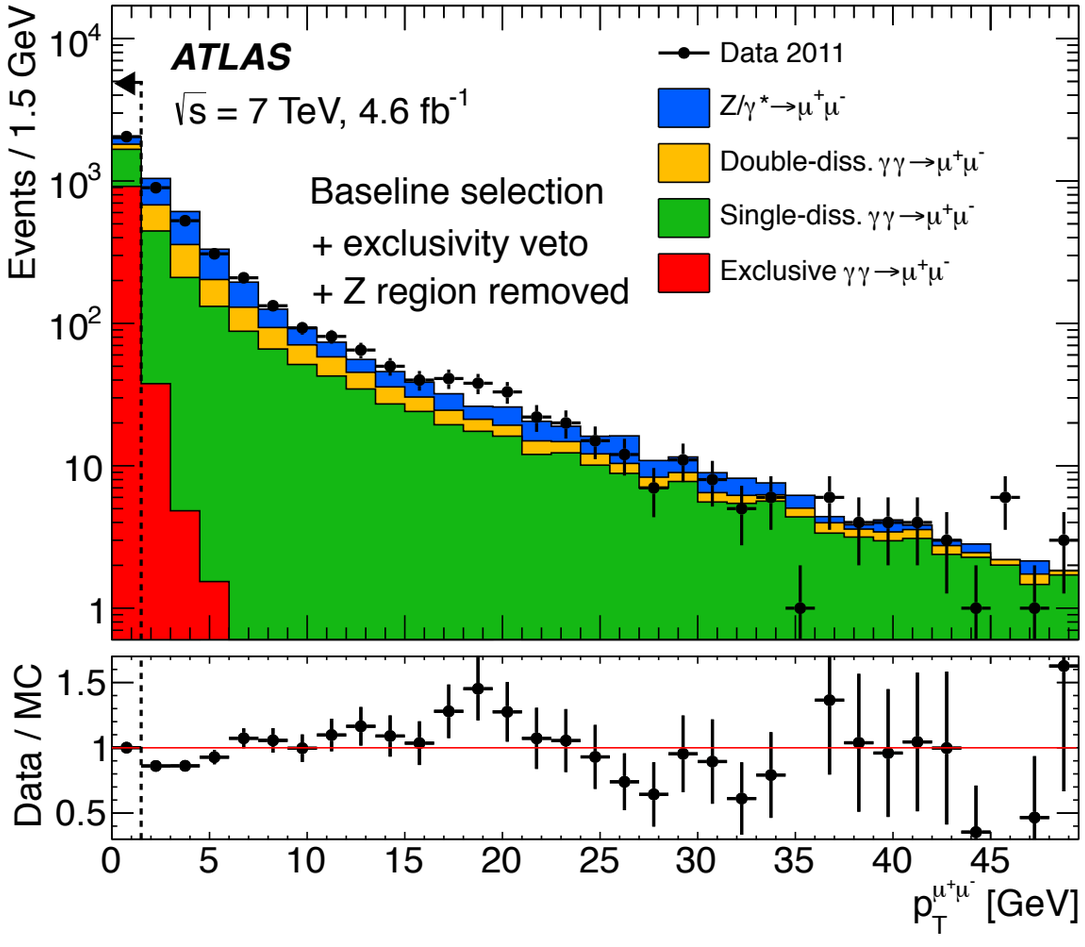

$\gamma\gamma \to \ell^+\ell^-$ *at 7 TeV*

Binned maximum-likelihood fit of the exclusive and SD contributions to measure the dilepton acoplanarity distribution (DD fixed to the MC predictions).

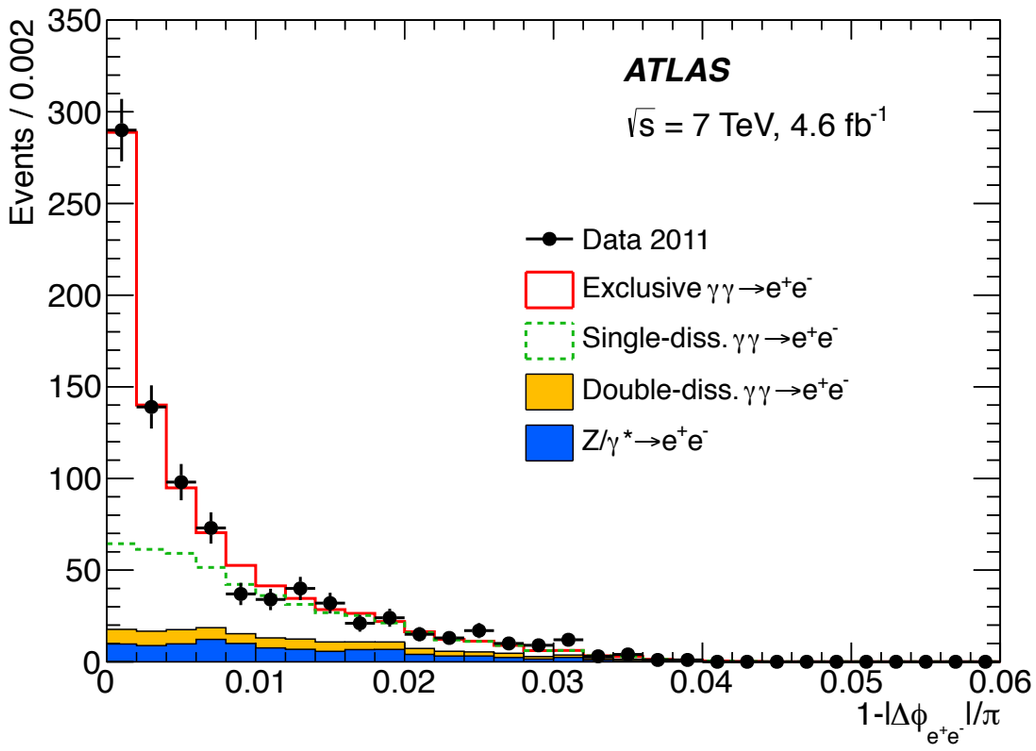

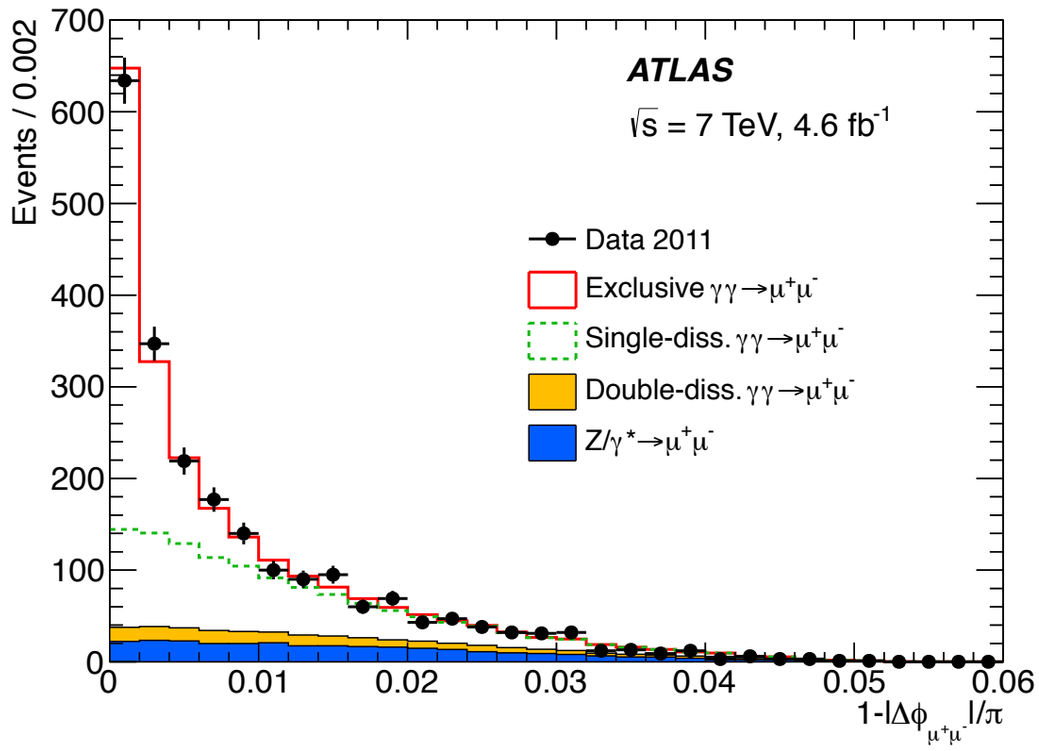

Theory prediction (QED-EPA) with the absorptive corrections (20%) (***PLB 741 (2015) 66-70***).

Measured cross section in agreement with the predictions corrected for absorptive effects. Good agreement with the CMS measurement (***JHEP 1201 (2012) 052***).

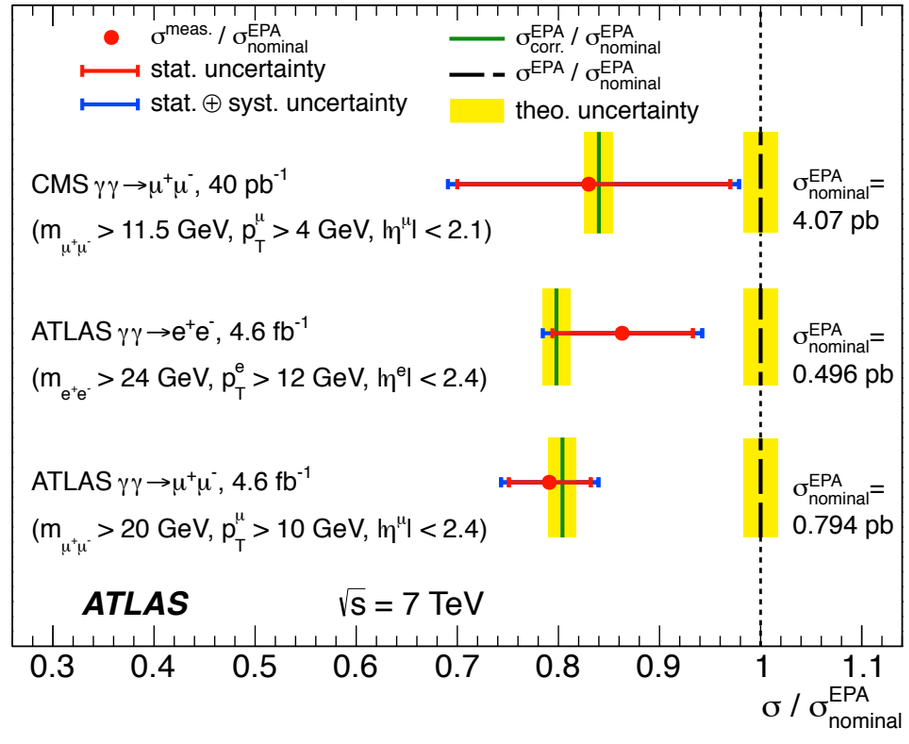

$\gamma\gamma \to \mu^+\mu^-$ *at 13 TeV*

Exclusive event selection:

- Exactly 2 tracks, veto on additional tracks with $\mathrm{p_T} > 0.4$ GeV, $|\eta| < 2.5$ and $z_0^{trk} < 1$ mm;
- $\mathrm{p_T}^{\ell\ell} < 1.5$ GeV;

Fiducial region

Invariant mass range	p_{T}^{μ} requirement	$\lvert\eta^{\mu}\rvert$ requirement
$12\ GeV < m_{\mu^+\mu^-} < 30\ GeV$	$> 6\ GeV$	< 2.4
$30\ GeV < m_{\mu^+\mu^-} < 70\ GeV$	$> 10\ GeV$	< 2.4

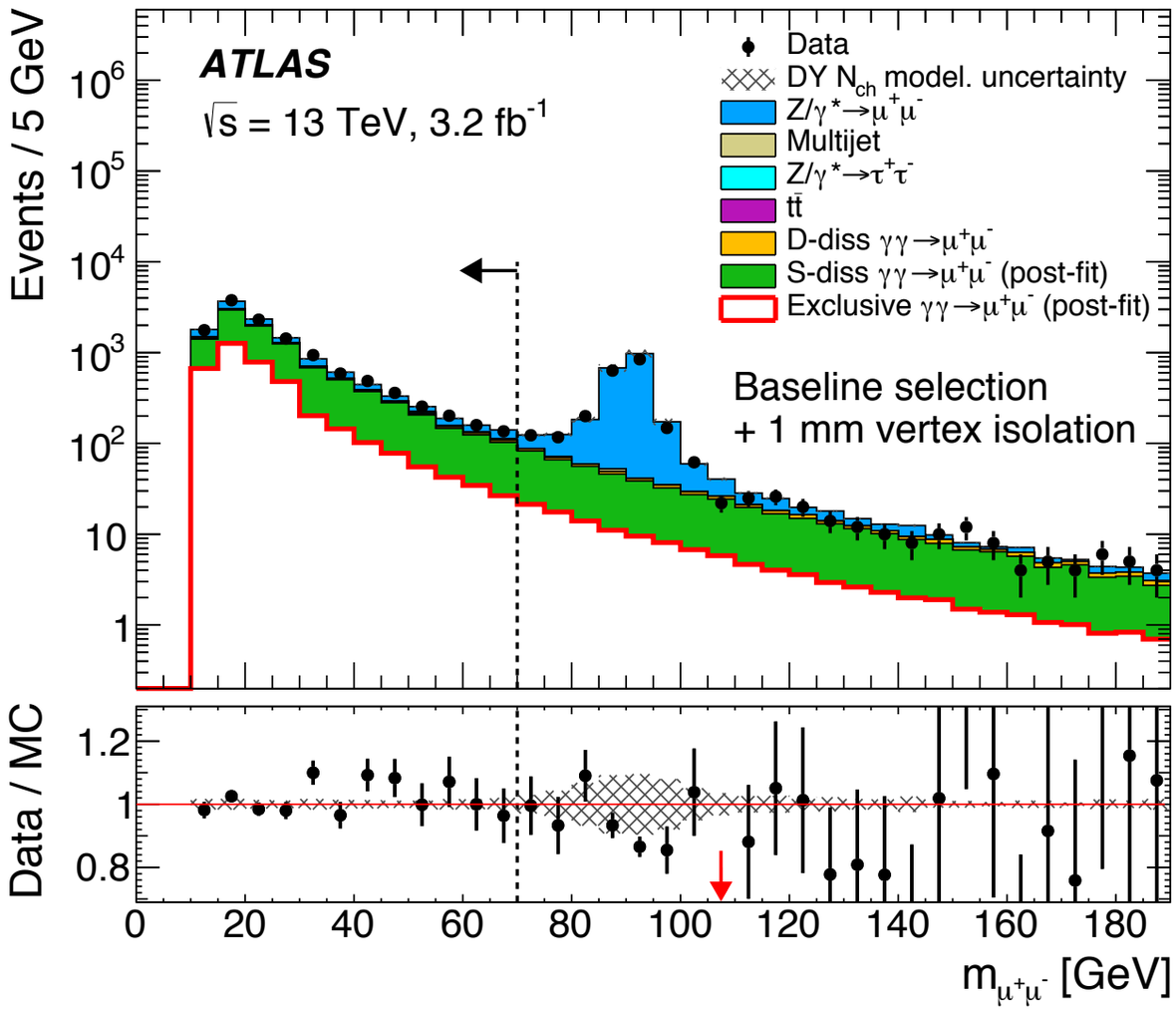

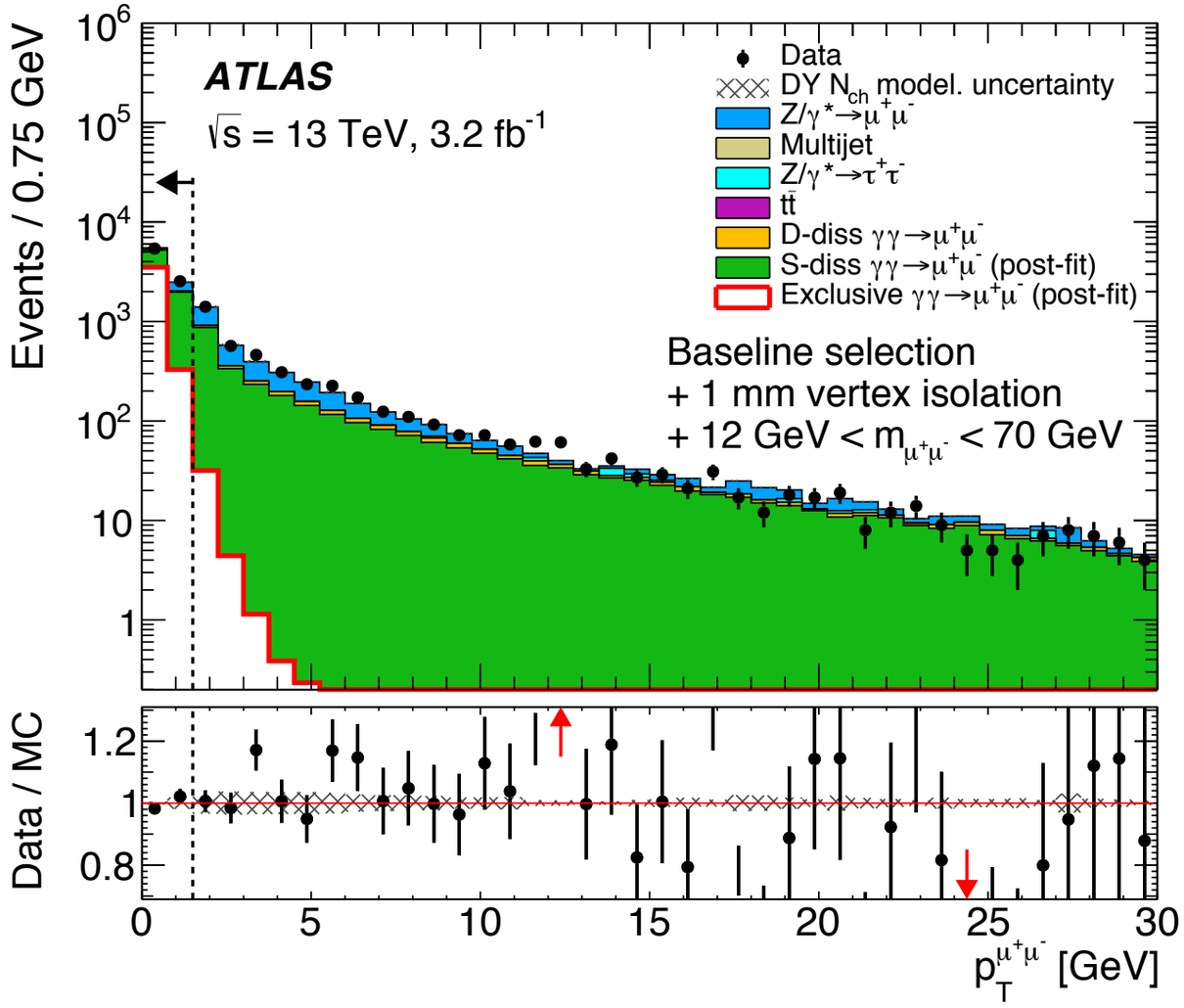

$\gamma\gamma \to \mu^+\mu^-$ *at 13 TeV*

Binned maximum-likelihood fit of the exclusive and SD contributions to measure the dimuon acoplanarity distribution.

EPA predictions (corrected for absorptive effects) in good agreement with measured cross section. SuperChic2 predictions poorly describe the data.

The precision of the measurements might improve by using dedicated forward proton detectors.

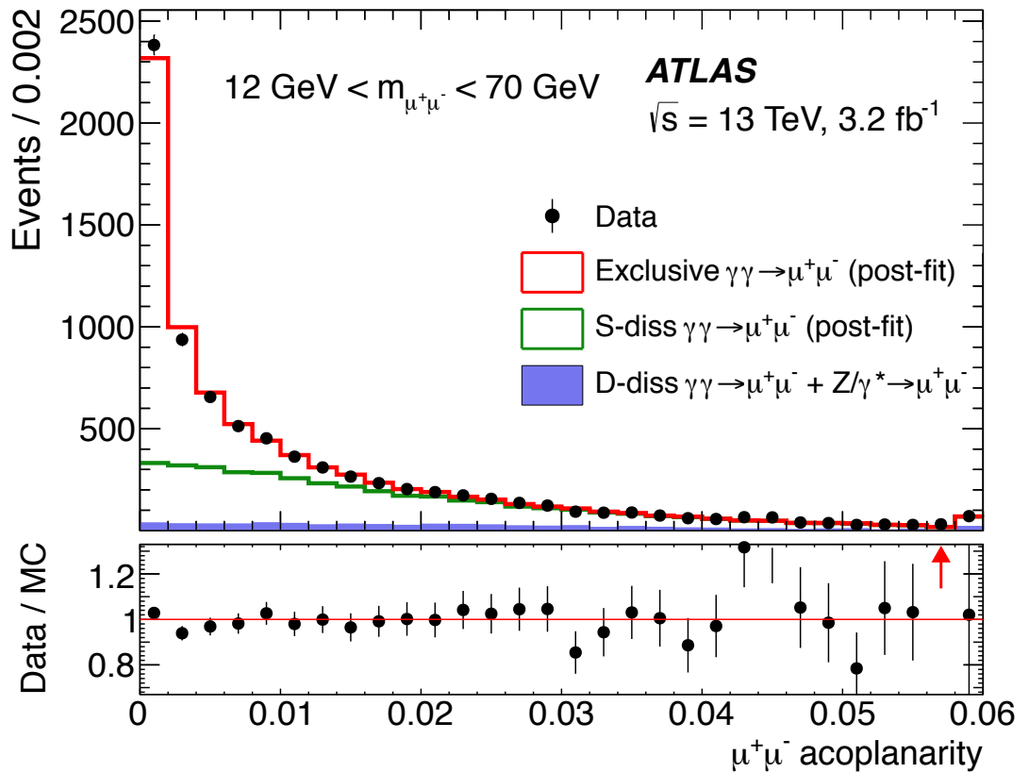

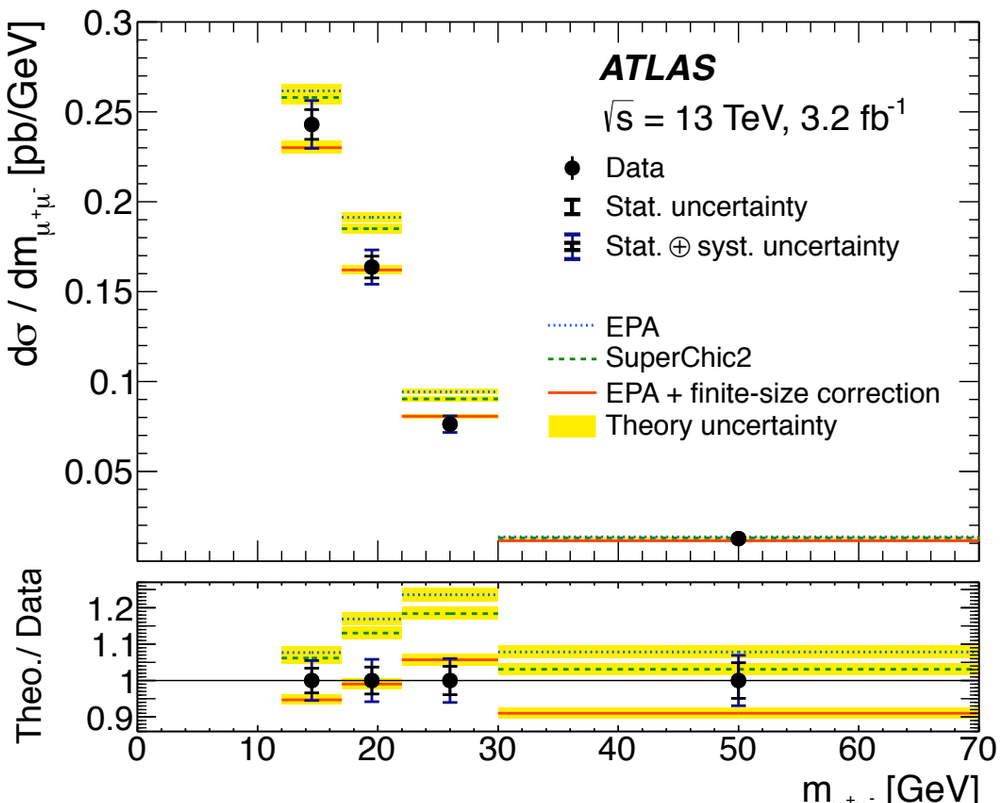

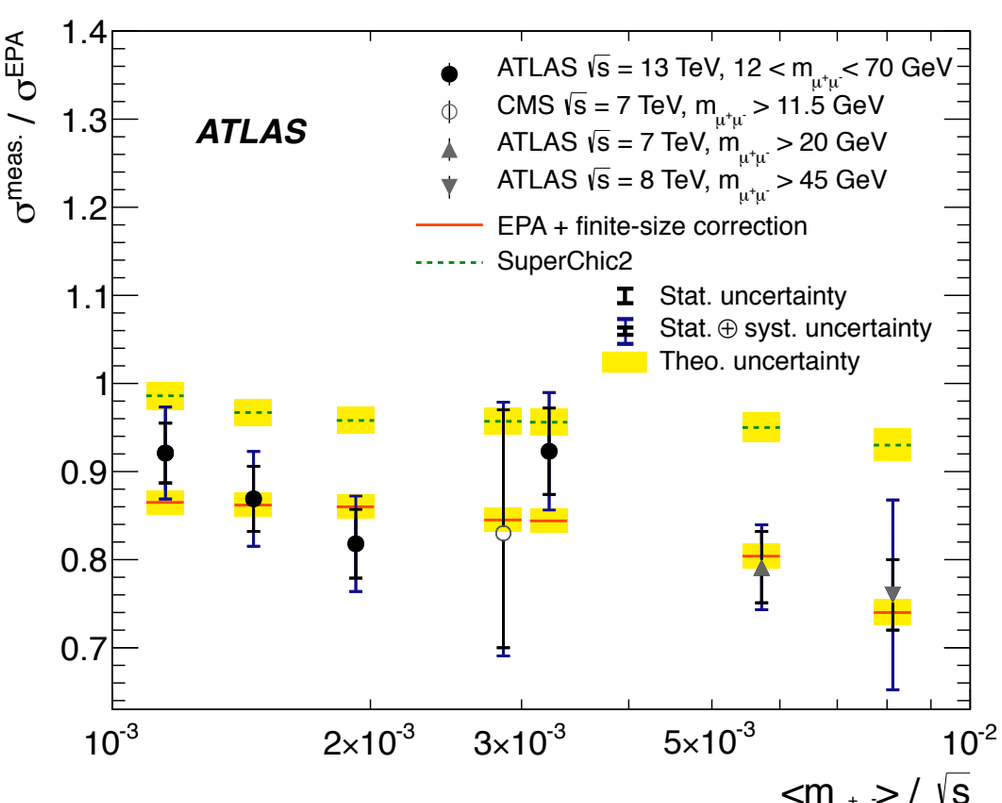

$\gamma\gamma \to W^+W^-$ *at 8 TeV*

- Test $\gamma\gamma WW$ quartic gauge coupling (QGC) and probe anomalous QGC (aQGC);
- Can be used for Higgs property studies;
- $WW \to e\nu\mu\nu$ final states are considered.

Veto on additional tracks with $\mathrm{p_T} > 0.4$ GeV
1 mm dilepton-vertex longitudinal isolation.

	W^+W^- selection	Higgs boson selection
Preselection	Oppositely charged $e\mu$ final states	
	$p_{\mathrm{T}}^{\ell 1} > 25\ GeV$ and $p_{\mathrm{T}}^{\ell 2} > 20\ GeV$	$p_{\mathrm{T}}^{\ell 1} > 25\ GeV$ and $p_{\mathrm{T}}^{\ell 2} > 15\ GeV$
	$m_{e\mu} > 20\ GeV$	$m_{e\mu} > 10\ GeV$
	$p_{\mathrm{T}}^{e\mu} > 30\ GeV$	
	Exclusivity selection, $\Delta z_0^{\mathrm{iso}}$	
aQGC signal	$p_{\mathrm{T}}^{e\mu} > 120\ GeV$	–
Spin-0 Higgs boson	–	$m_{e\mu} < 55\ GeV$
	–	$\Delta\phi_{e\mu} < 1.8$
	–	$m_{\mathrm{T}} < 140$ GeV

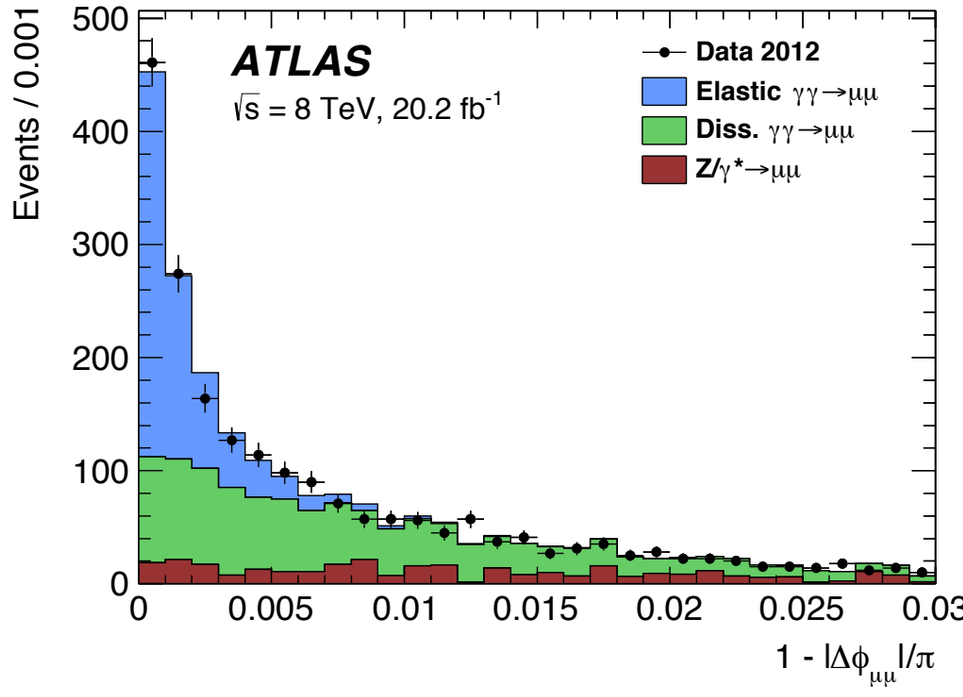

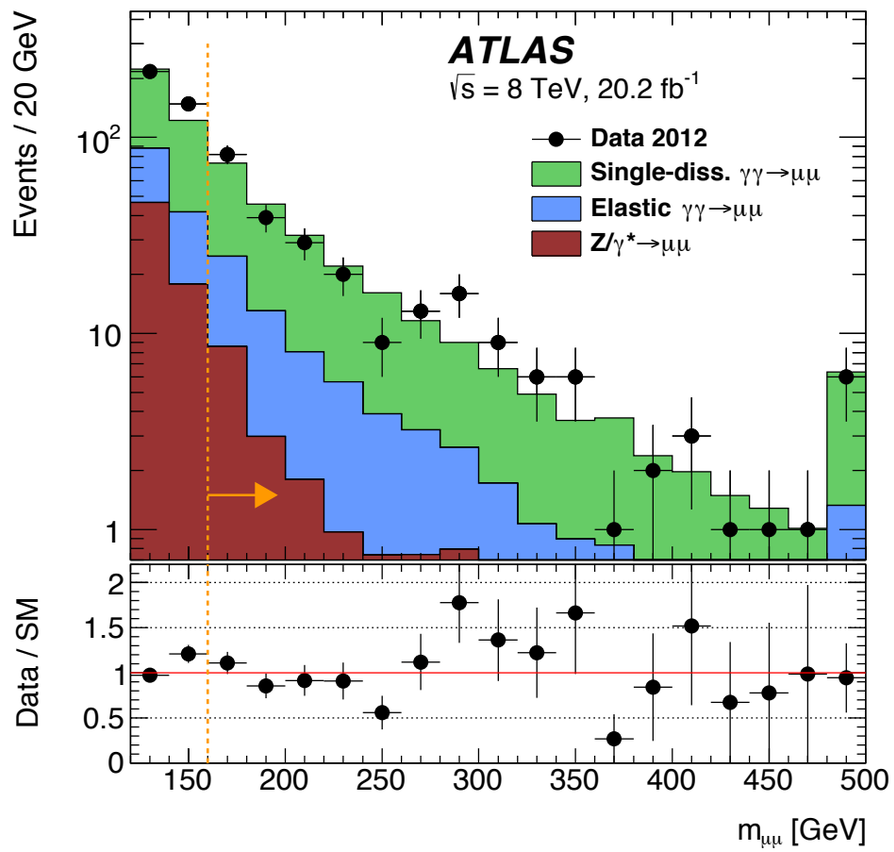

Validation on the exclusivity selection using the exclusive dilepton production. Ratio of observed elastic $\gamma\gamma \to \ell^+\ell^-$ to EPA predictions ~ 0.76. Correction factor for $m_{\ell\ell} > 160$ GeV to take into account the lack of simulations for dissociative events (~3.3).

$\gamma\gamma \to W^+W^-$ at 8 TeV

	Expected Signal	Data	Total Bkg	Incl W^+W^-	Excl. $\tau\tau$	Other-VV	Other Bkg	SM/Data	ϵA (Signal)
Preselection	22.6 ± 1.9	99424	97877	11443	21.4	1385	85029	0.98	0.254
$p_{\mathrm{T}}^{\ell\ell} > 30$ GeV	17.6 ± 1.5	63329	63023	8072	4.30	896.3	54051	1.00	0.198
$\Delta z_0^{\mathrm{iso}}$ requirement	9.3 ± 1.2	23	8.3 ± 2.6	6.6 ± 2.5	1.4 ± 0.3	0.3 ± 0.2	–	0.77	0.105 ± 0.012
aQGC signal region									
$p_{\mathrm{T}}^{\ell\ell} > 120$ GeV	0.37 ± 0.04	1	0.37 ± 0.13	0.32 ± 0.12	0.05 ± 0.03	0	–	0.74	0.0042 ± 0.0005

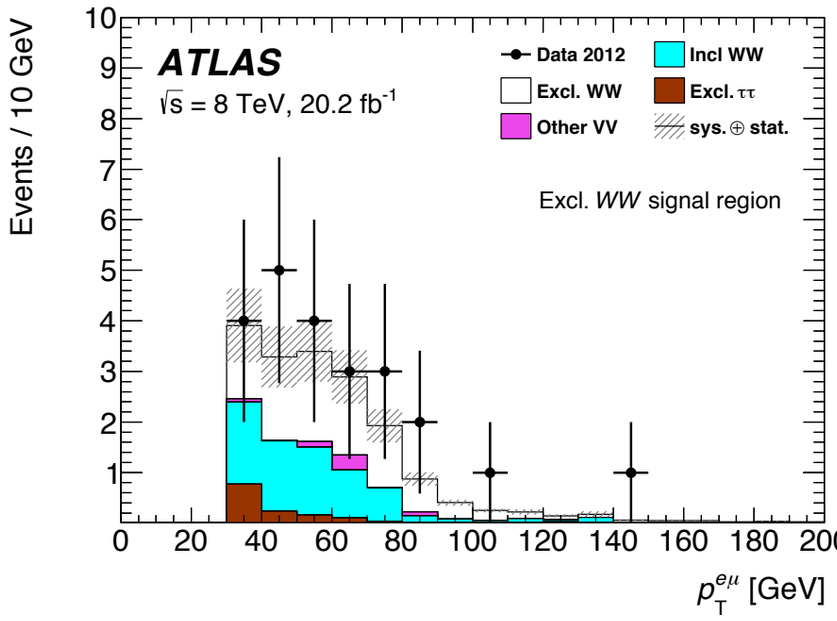

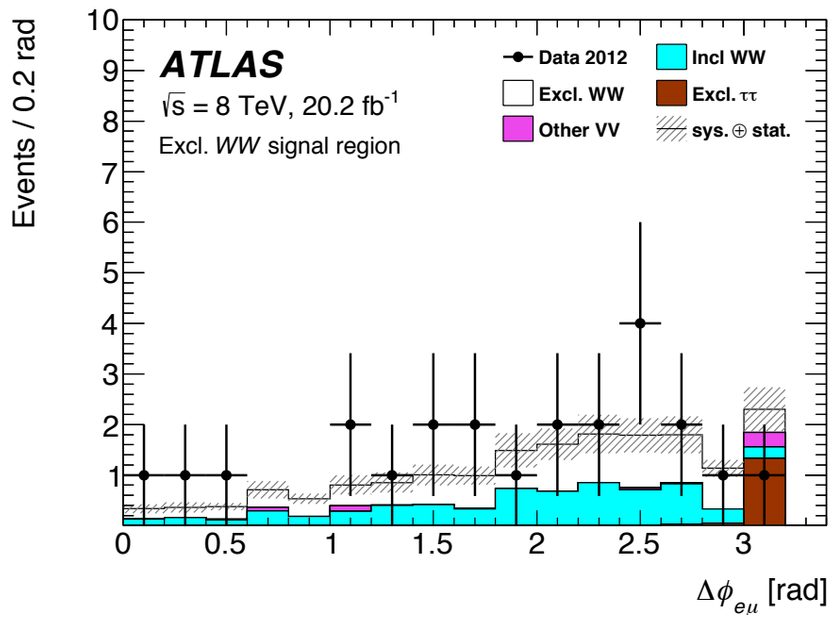

Measurement significance of $3\,\sigma$.
Additional cut on $\mathrm{p_T}^{e\mu}$ to enhance the aQGC contribution. New limits set.

Coupling	$\Lambda_{\mathrm{cutoff}}$	Observed allowed range [GeV^{-2}]	Expected allowed range [GeV^{-2}]
a_0^W/Λ^2	500 GeV	$[-0.96 \times 10^{-4},\ 0.93 \times 10^{-4}]$	$[-0.90 \times 10^{-4},\ 0.87 \times 10^{-4}]$
a_C^W/Λ^2	500 GeV	$[-3.5 \times 10^{-4},\ 3.3 \times 10^{-4}]$	$[-3.3 \times 10^{-4},\ 3.1 \times 10^{-4}]$
a_0^W/Λ^2	∞	$[-1.7 \times 10^{-6},\ 1.7 \times 10^{-6}]$	$[-1.5 \times 10^{-6},\ 1.6 \times 10^{-6}]$
a_C^W/Λ^2	∞	$[-6.4 \times 10^{-6},\ 6.3 \times 10^{-6}]$	$[-5.9 \times 10^{-6},\ 5.8 \times 10^{-6}]$

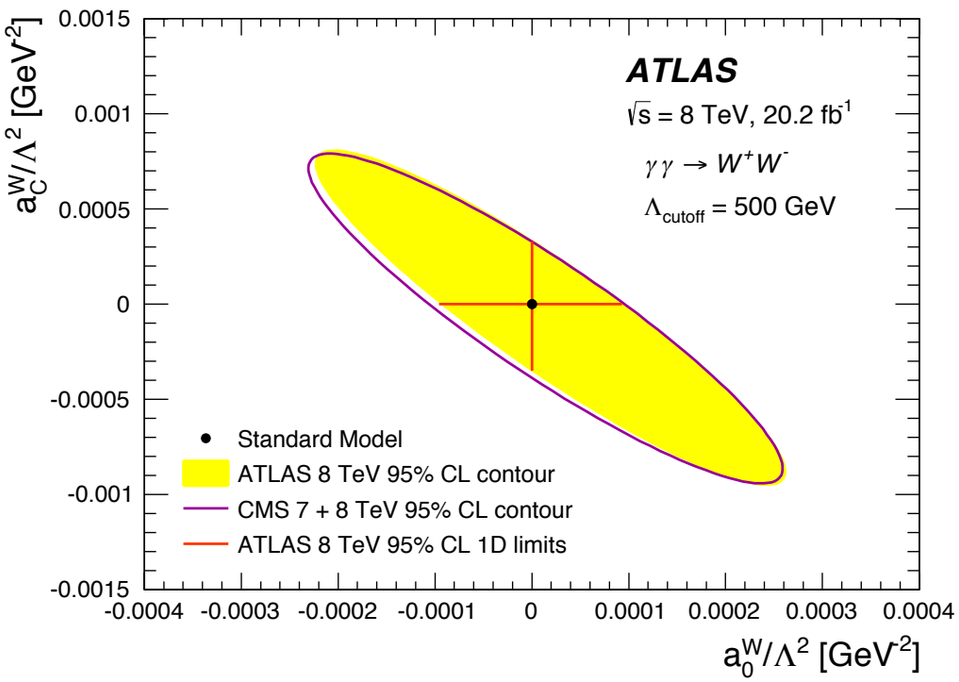

Powerful channel for aQGC constraints on the $\gamma\gamma WW$ quartic coupling vertex.

https://twiki.cern.ch/twiki/bin/view/CMSPublic/PhysicsResultsSMPaTGC

Summary and Conclusions

→ The enhanced like-sign production at low Q (Bose-Einstein effect) is attributed to ordered hadron-chains with mass below 591^{+8}_{-13}MeV.

Jets

→ The results of the soft-drop measurements are the first pp data that are compared to a calculation with precision beyond PS.

→ The inclusive jet analysis can be used to constraint the PDFs;

→ First comparison of the measured cross sections with NNLO at 13 TeV;

→ First measurement of dijet cross sections at 13 TeV;

Exclusive production

→ Cross section of the exclusive dilepton production consistent with the (20%) suppression expected due to the proton absorption contributions.

→ Evidence of the exclusive W^+W^- production (significance $3\,\sigma$). Lower threshold on tracks veto may improve the future results.

→ No evidence of aQGC.

→ Looking forward to repeat the measurement using forward detectors.

THANK YOU FOR YOUR ATTENTION!

BACKUP

Bose-Einstein Correlations (BEC)

- Correlation between identical bosons;
- Probe of the space-time geometry of the hadronisation region;
- Allow the determination of the properties of the source.

$$C_2(Q) = \frac{\rho(Q)}{\rho_0(Q)} = C_0[1 + \Omega(\lambda, QR)](1 + \epsilon Q) \text{ where } \begin{array}{l} \Omega^G(\lambda) = \lambda \cdot e^{-R^2Q^2} \\ \Omega^E(\lambda) = \lambda \cdot e^{-RQ} \end{array}$$

$$R_2(Q) = \frac{C_2^{Data}}{C_2^{MC}} \longrightarrow$$ Eliminates the problems with energy-momentum conservations, topology, resonances, etc.

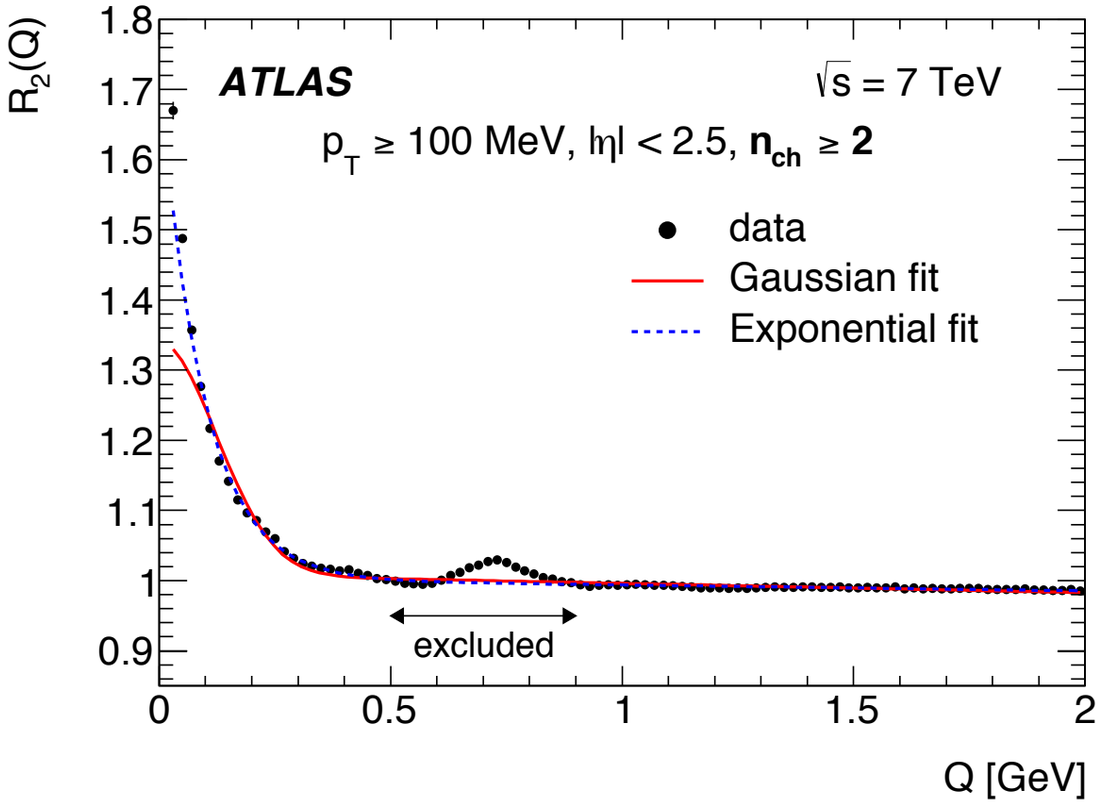

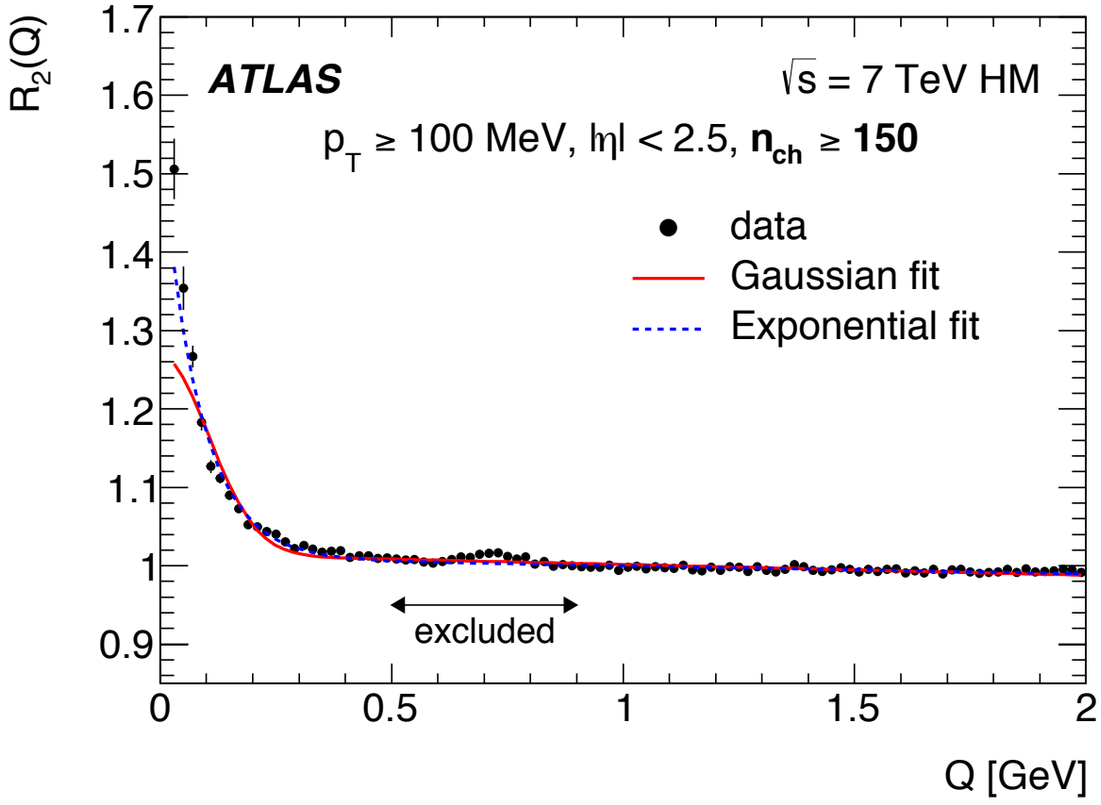

- Mismodelling in MC at $Q \sim 0.7$ GeV $\longrightarrow 0.5 \leq Q \leq 0.9$ GeV excluded from the fit;
- The exponential fit describes better than the Gaussian fit the low Q region (enhanced of BEC).

Bose-Einstein Correlations

The λ decrease with multiplicity is well described by the exponential fit.
R increases with multiplicity up to n_{ch}, independently of the center-of-mass energy.
Good agreement with the CMS and UA1 measurements.

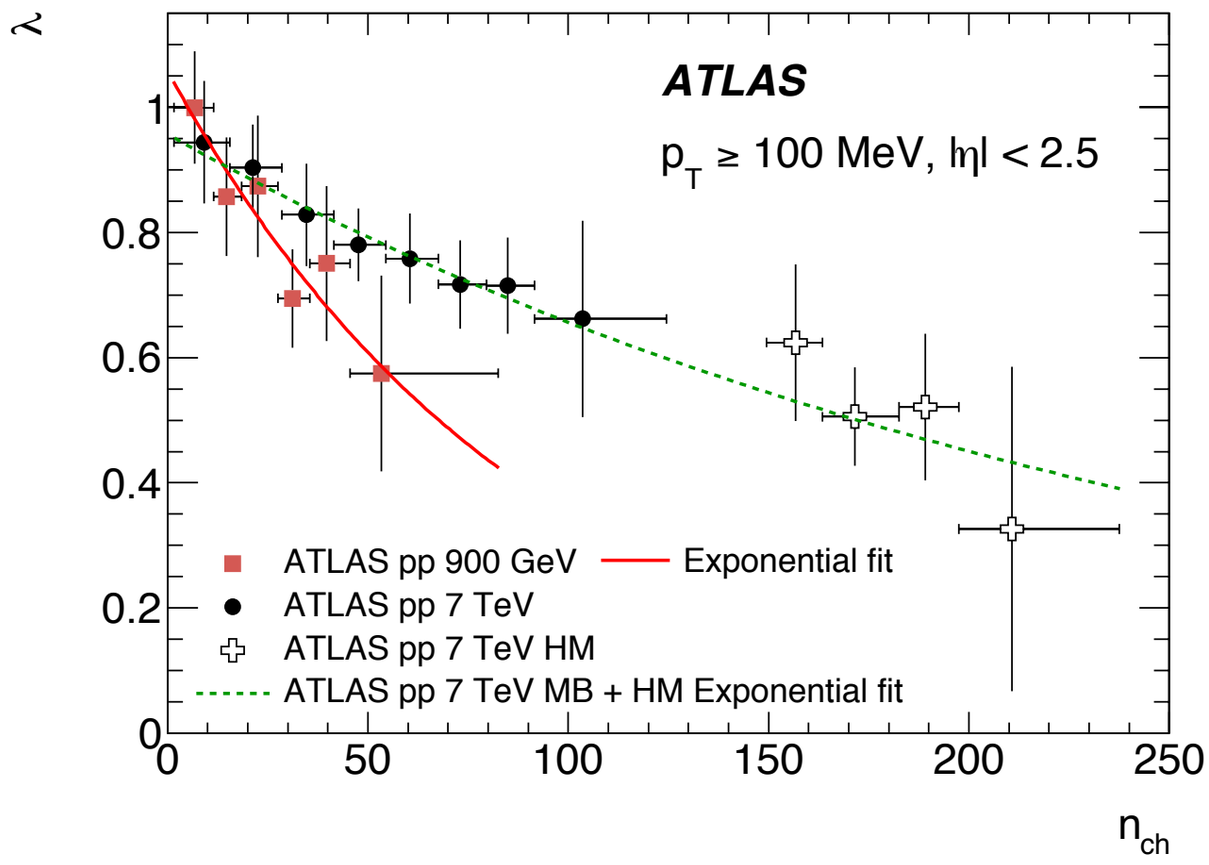

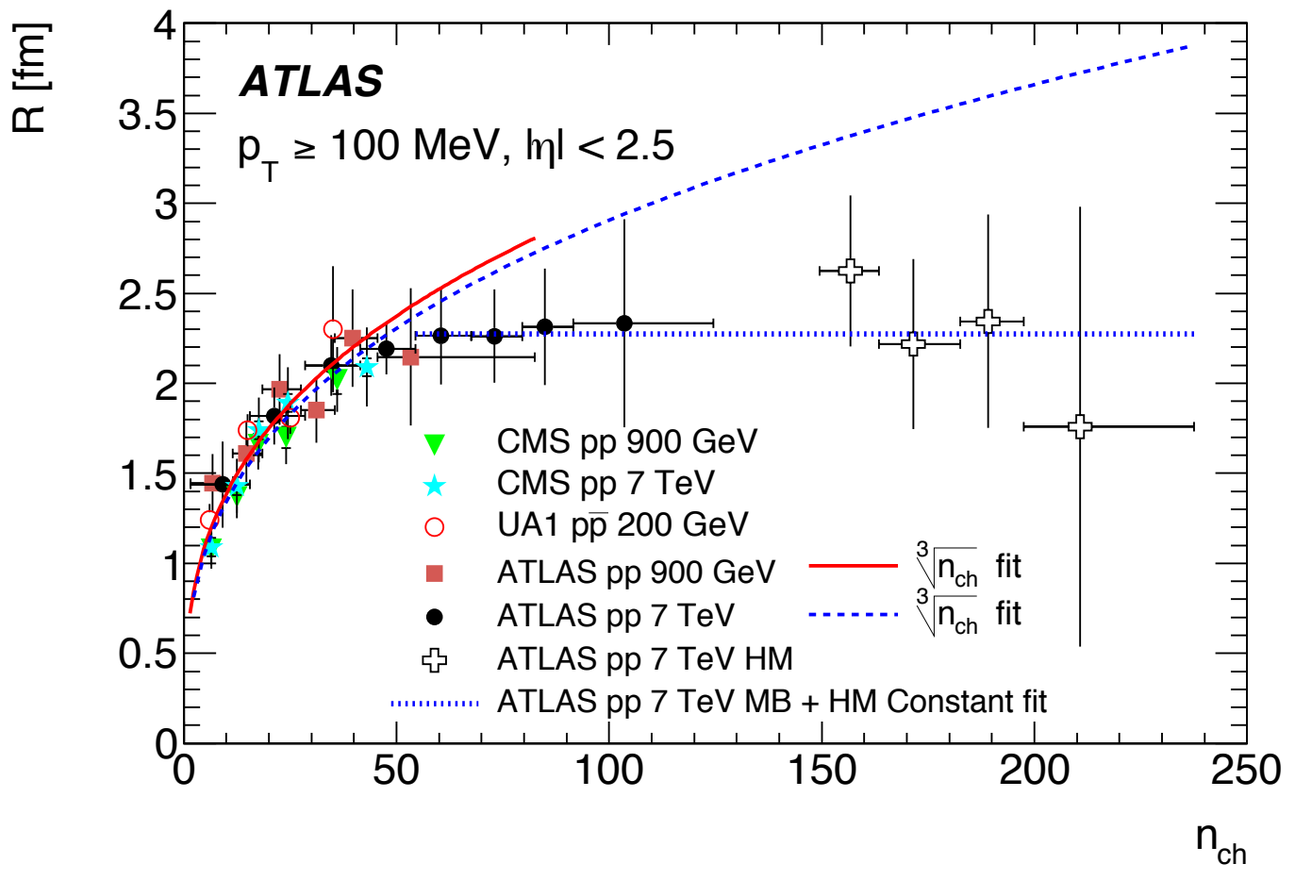

The saturation of R is expected in a Pomeron-based model as consequence of the overlap of colliding protons at $n_{ch} \approx 70$, as observed in this study!
However, the same model predicts that above 70, R decreases with multiplicity.

Soft-drop algorithm

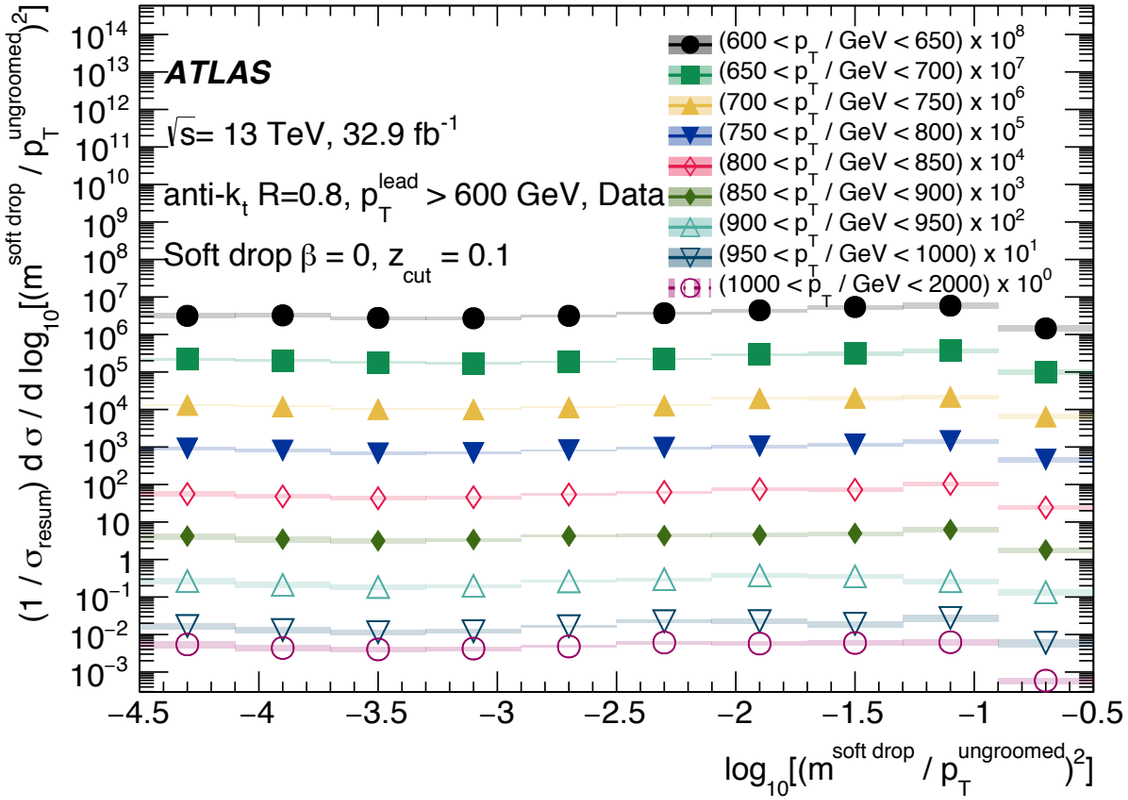

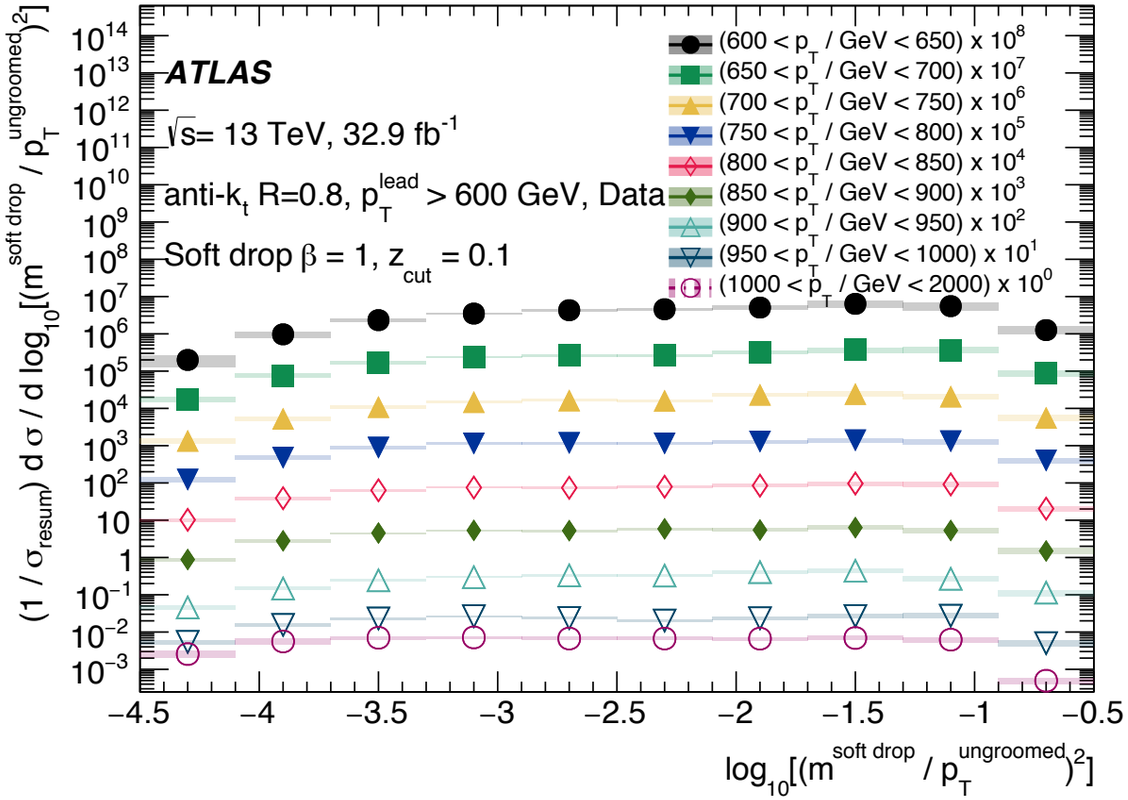

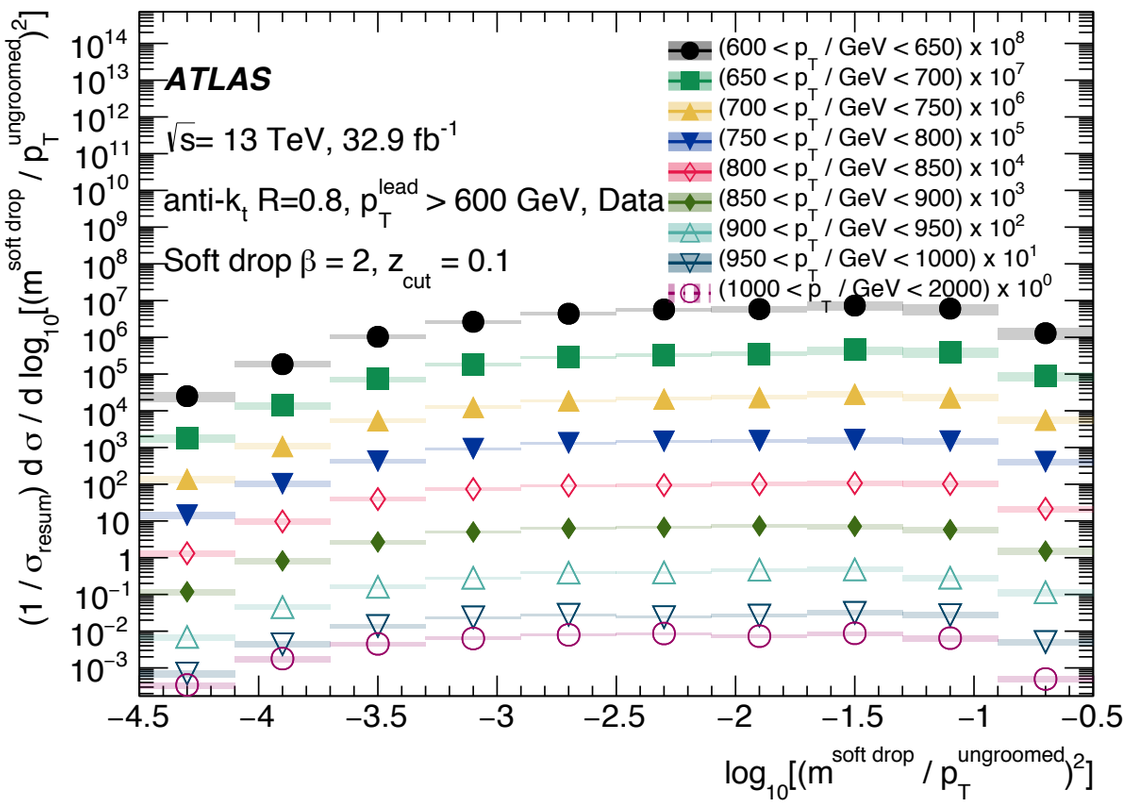

Inclusive Jet production

$\sqrt{s} = 8$ TeV $\sqrt{s} = 13$ TeV

- The dominant experimental uncertainties are the jet energy scale and jet energy resolution.
- Theory predictions corrected for non-perturbative and electroweak effects.

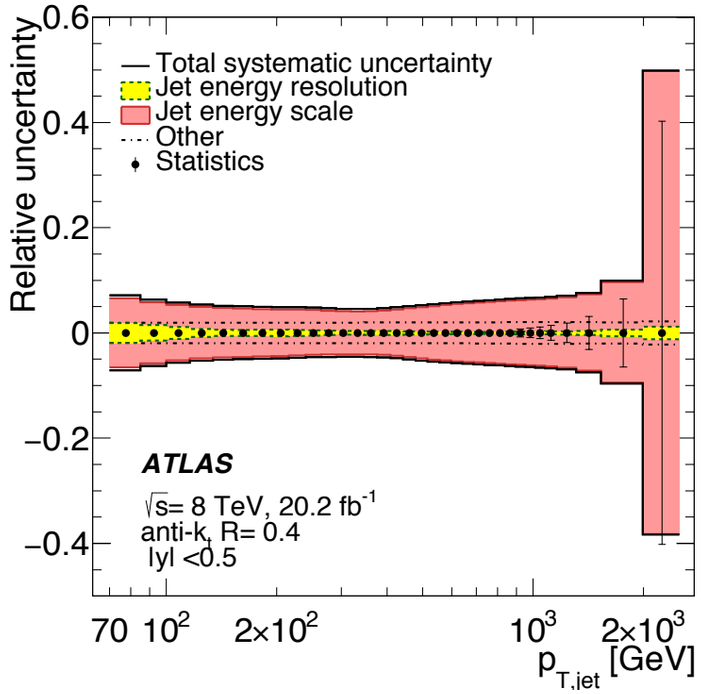

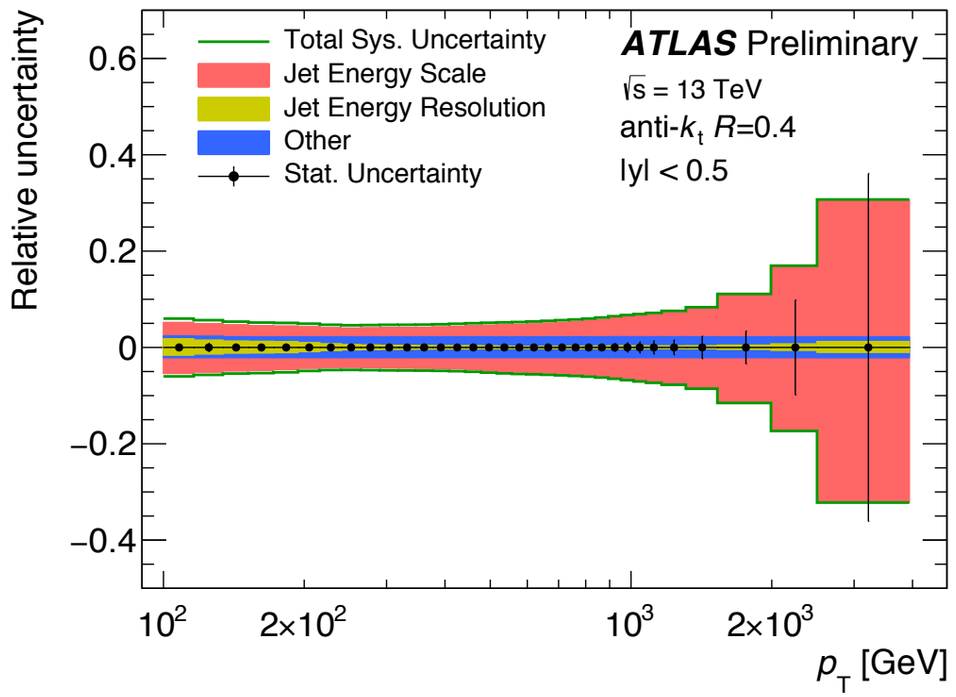

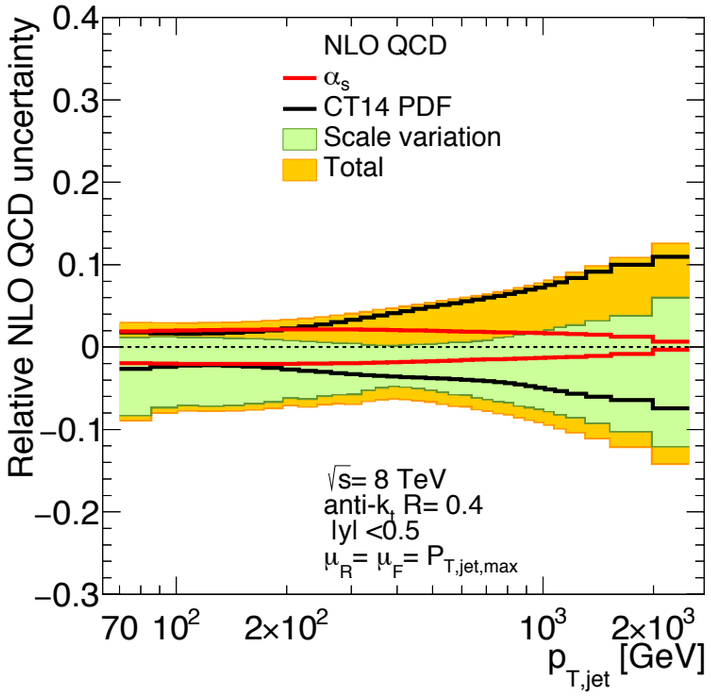

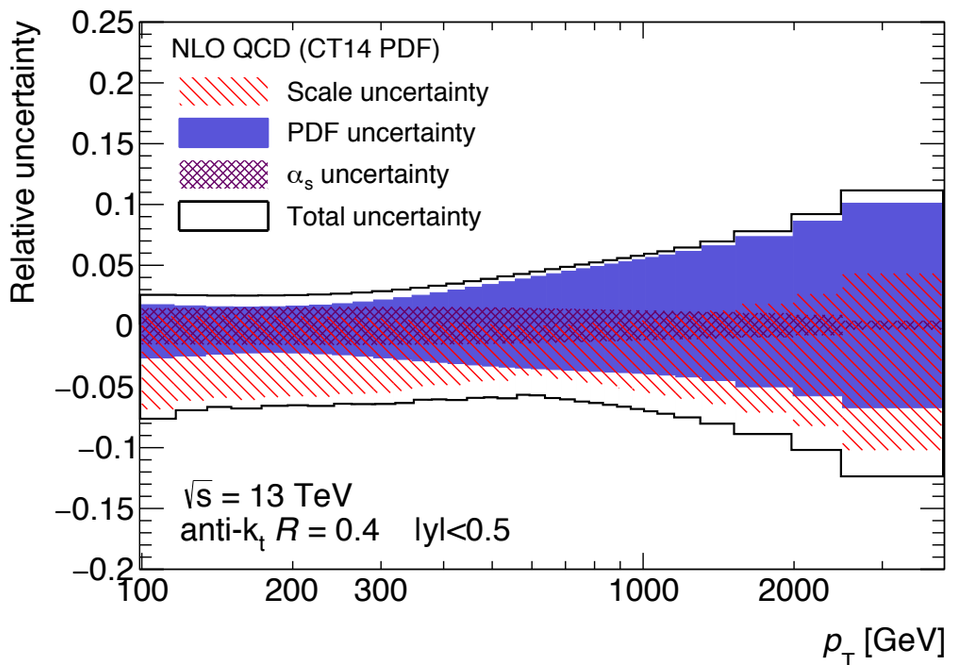

Inclusive Jet production

$\sqrt{s} = 8$ TeV

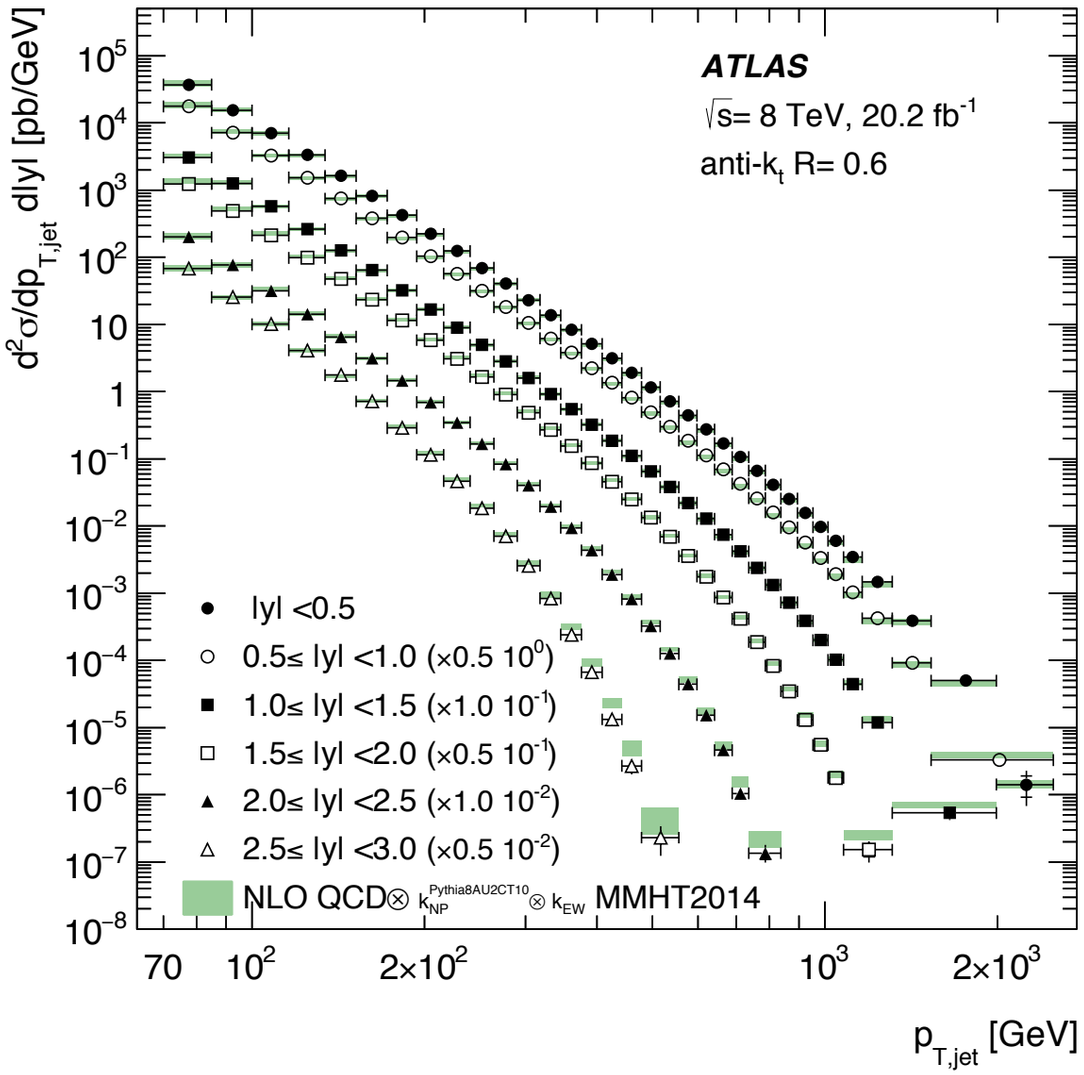

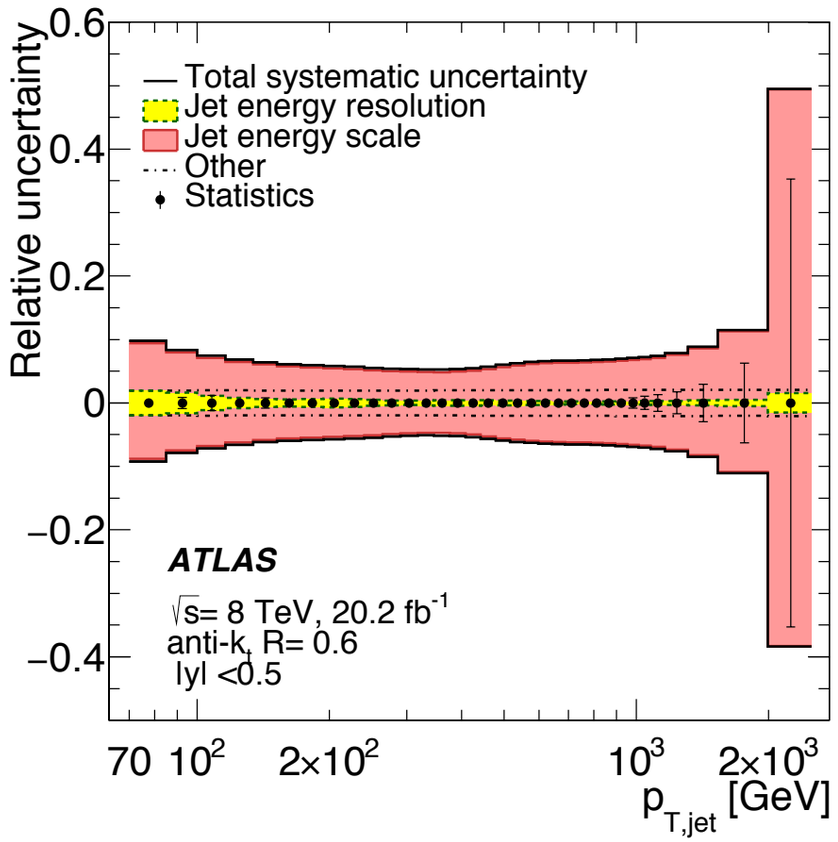

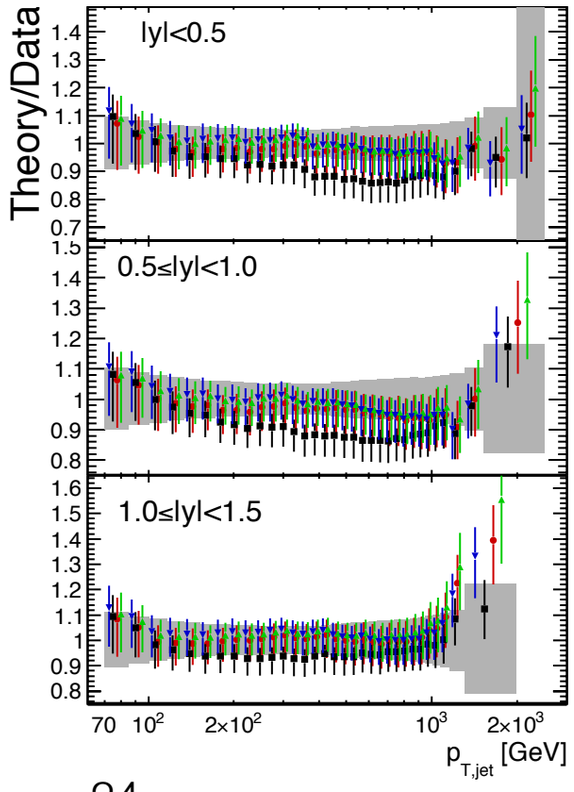

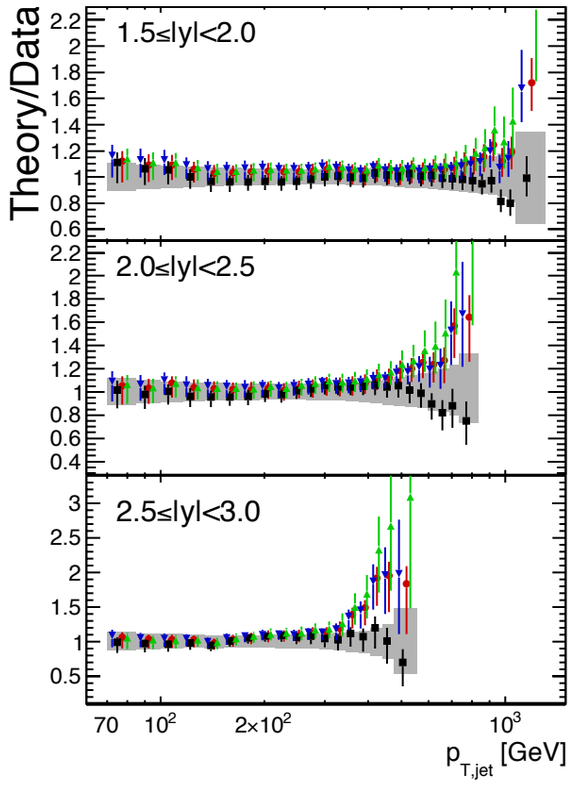

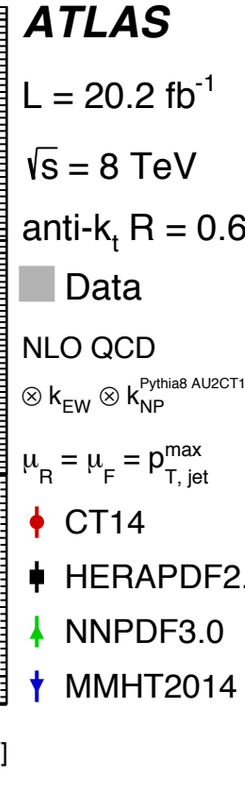

Inclusive jet production at 13 TeV

Summary of the p-values obtained from the comparison of the inclusive jet cross section and the NLO pQCD predictions for various PDFs and for each y^* bin.

	P_{obs}				
Rapidity ranges	CT14	MMHT 2014	NNPDF 3.0	HERAPDF 2.0	ABMP16
$p_{\text{T}}^{\text{max}}$					
$\lvert y\rvert < 0.5$	67%	65%	62%	31%	50%
$0.5 \leq \lvert y\rvert < 1.0$	5.8%	6.3%	6.0%	3.0%	2.0%
$1.0 \leq \lvert y\rvert < 1.5$	65%	61%	67%	50%	55%
$1.5 \leq \lvert y\rvert < 2.0$	0.7%	0.8%	0.8%	0.1%	0.4%
$2.0 \leq \lvert y\rvert < 2.5$	2.3%	2.3%	2.8%	0.7%	1.5%
$2.5 \leq \lvert y\rvert < 3.0$	62%	71%	69%	25%	55%
$p_{\text{T}}^{\text{jet}}$					
$\lvert y\rvert < 0.5$	69%	67%	66%	30%	46%
$0.5 \leq \lvert y\rvert < 1.0$	7.4%	8.9%	8.6%	3.4%	2.0%
$1.0 \leq \lvert y\rvert < 1.5$	69%	62%	68%	45%	54%
$1.5 \leq \lvert y\rvert < 2.0$	1.3%	1.6%	1.4%	0.1%	0.5%
$2.0 \leq \lvert y\rvert < 2.5$	8.7%	6.6%	7.4%	1.0%	3.6%
$2.5 \leq \lvert y\rvert < 3.0$	65%	72%	72%	28%	59%

Inclusive Jet production

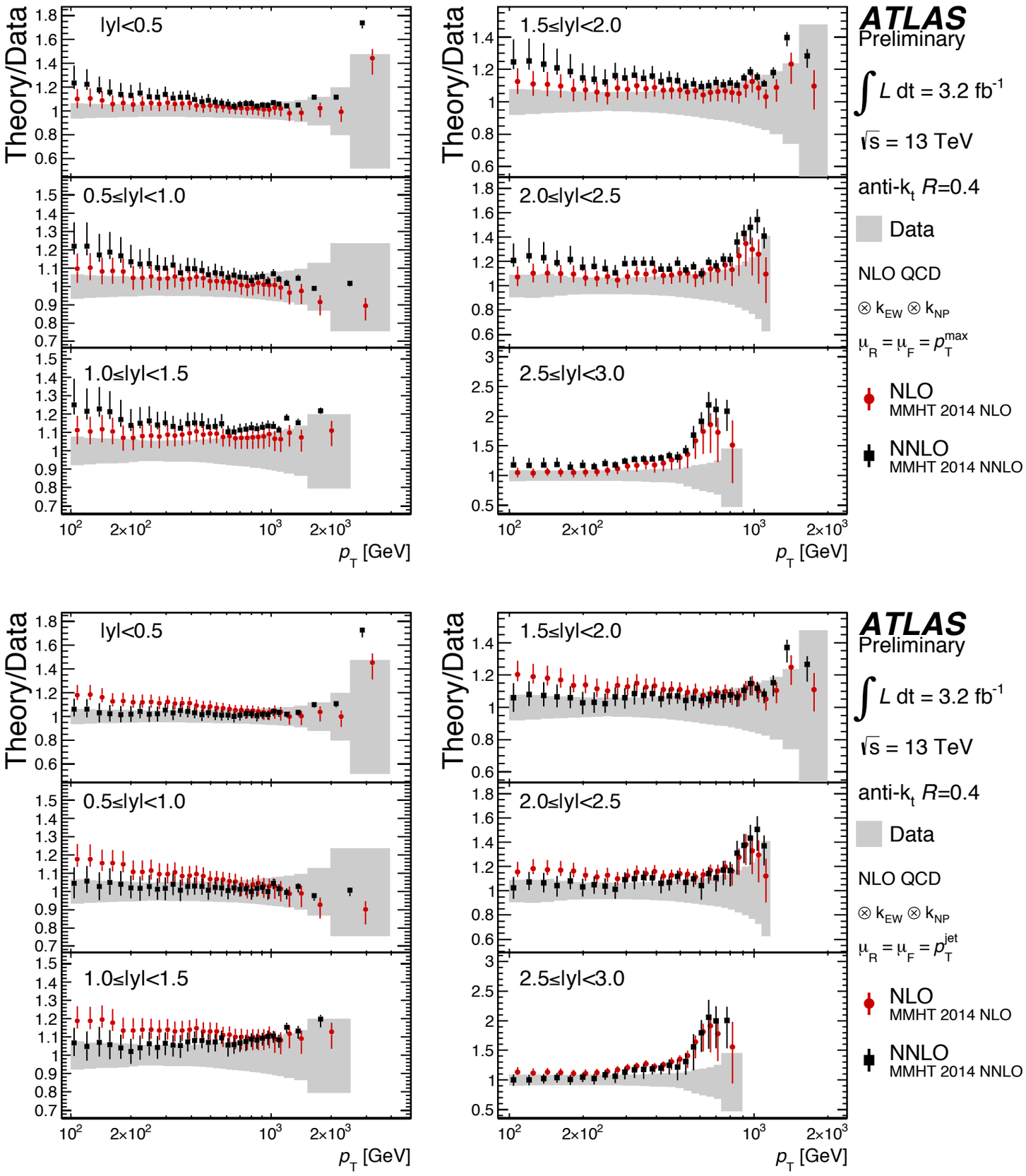

The differences between the two predictions are in agreement within the scale uncertainties.

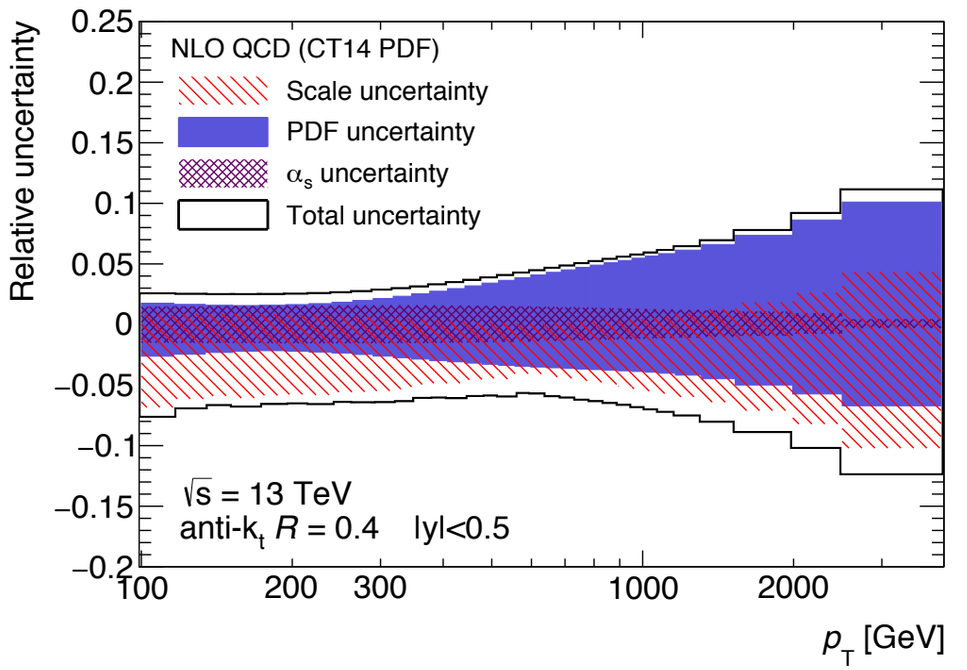

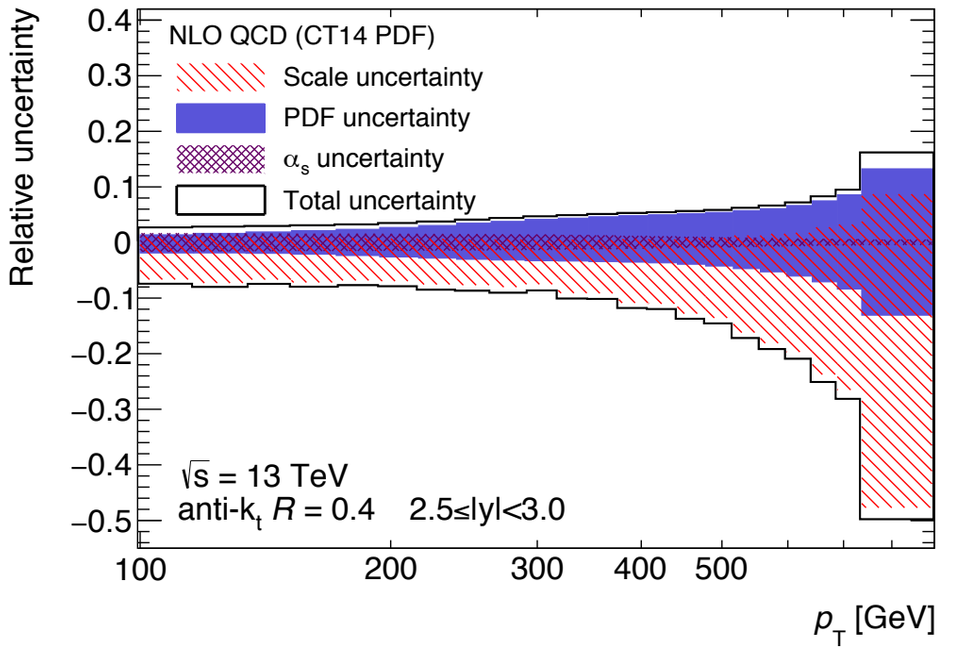

Dijet production at 13 TeV

- At least two jets with $P_T > 75$ GeV, within the interval $|y| < 3$;
- $H_{T,2} = P_{T1} + P_{T2}$ has to be higher than 200 GeV;

Double differential cross section is measured as a function of the invariant mass of the dijet system, m_{jj}, in $y^* = |y_1 - y_2|/2$ bins.

Experimental uncertainties around 5% until 1 TeV, then they rise to 30% at high m_{jj}.

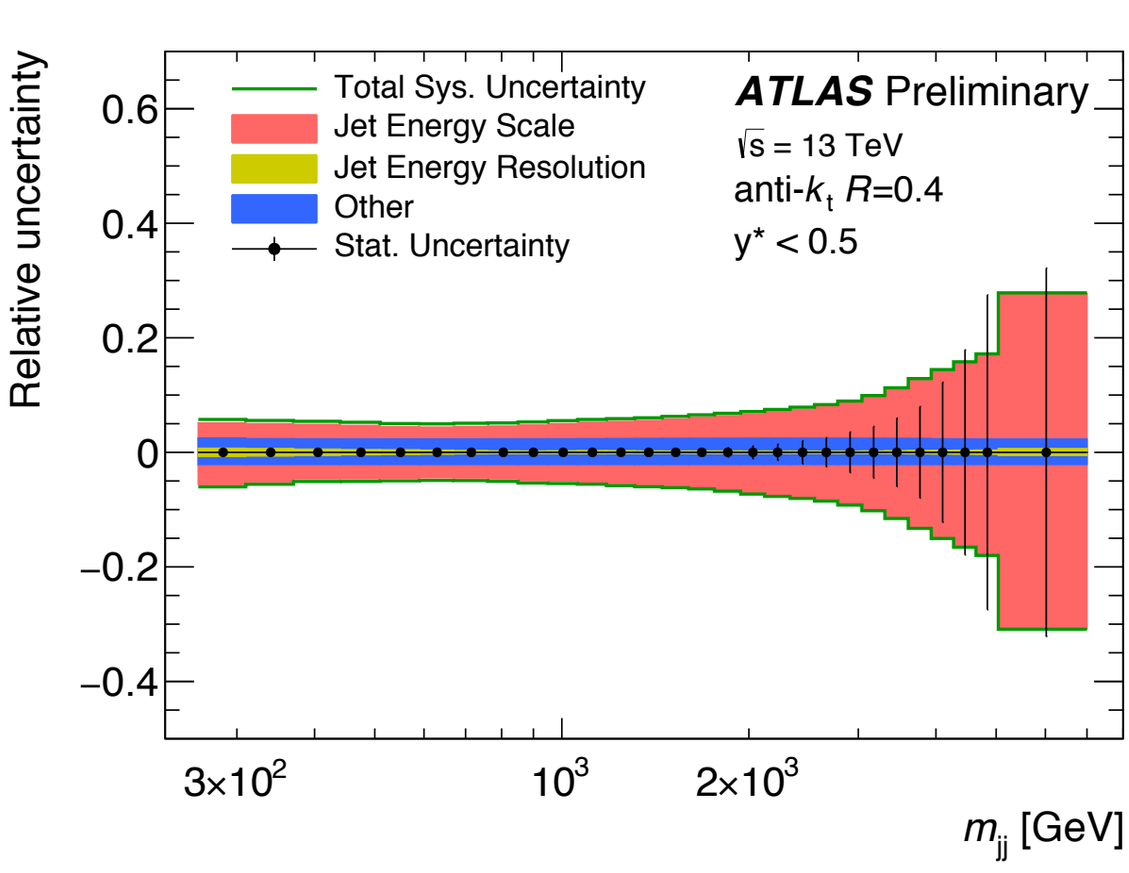

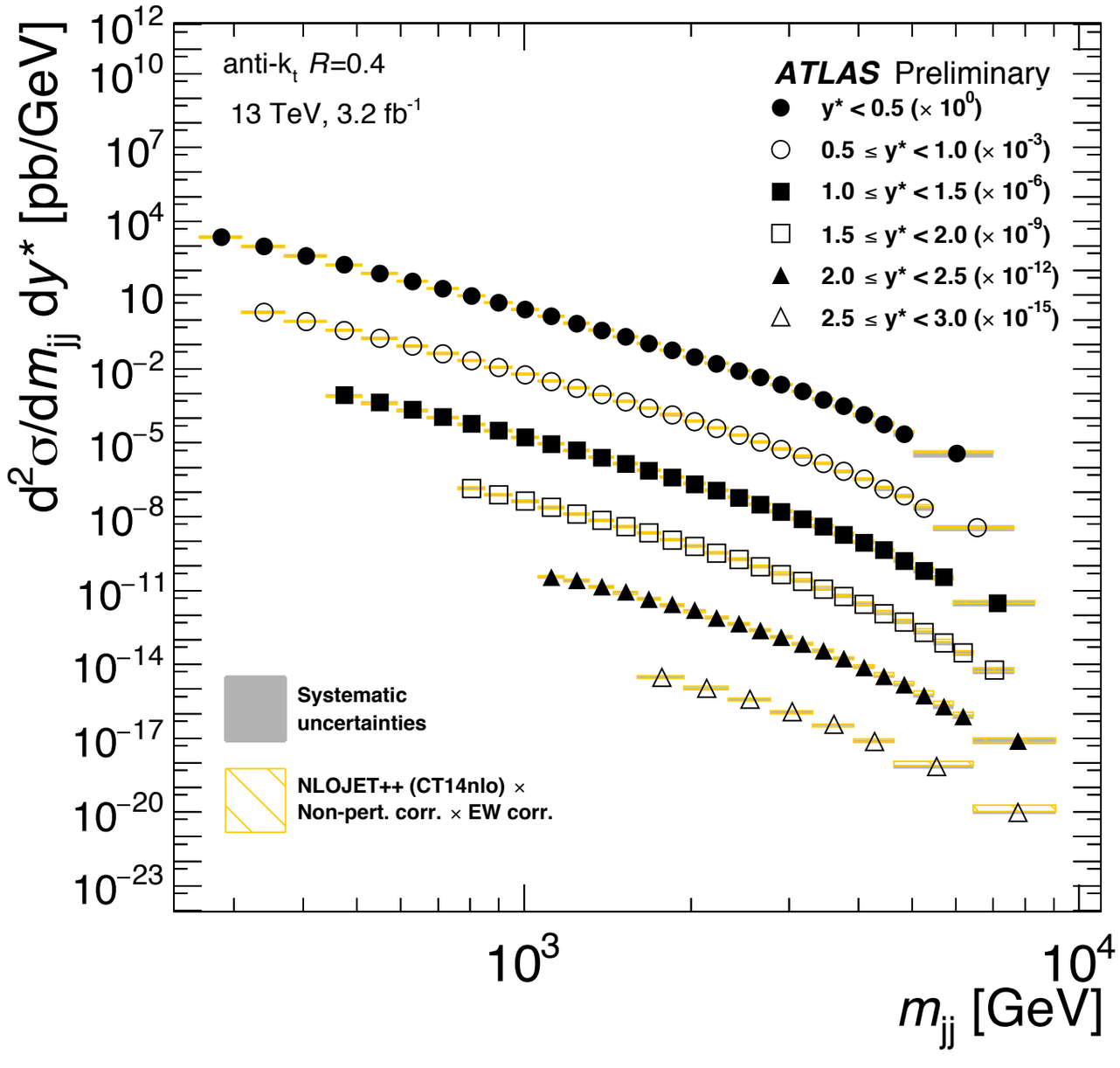

Di-Jet production at 13 TeV

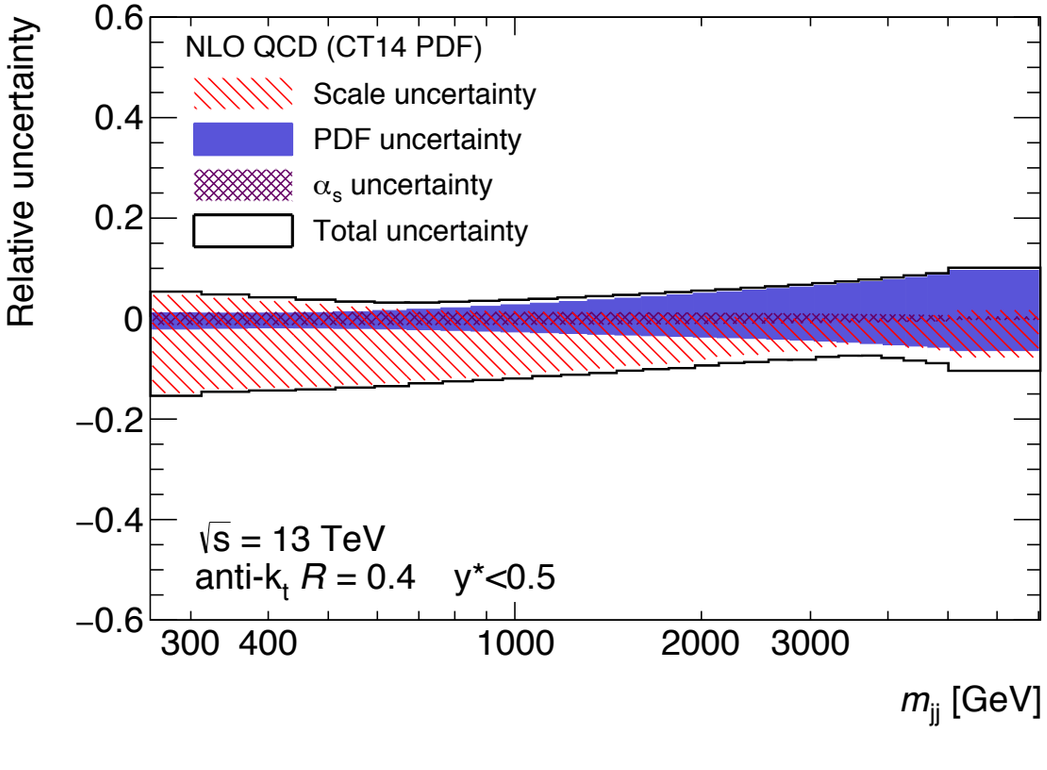

Fair agreement between data and NLO QCD predictions within the experimental uncertainties.

χ^2 tests made for each PDF set in individual m_{jj} and y^* bins and when fitting to all y^* regions (see backup). Good agreement between NLO QCD and data.

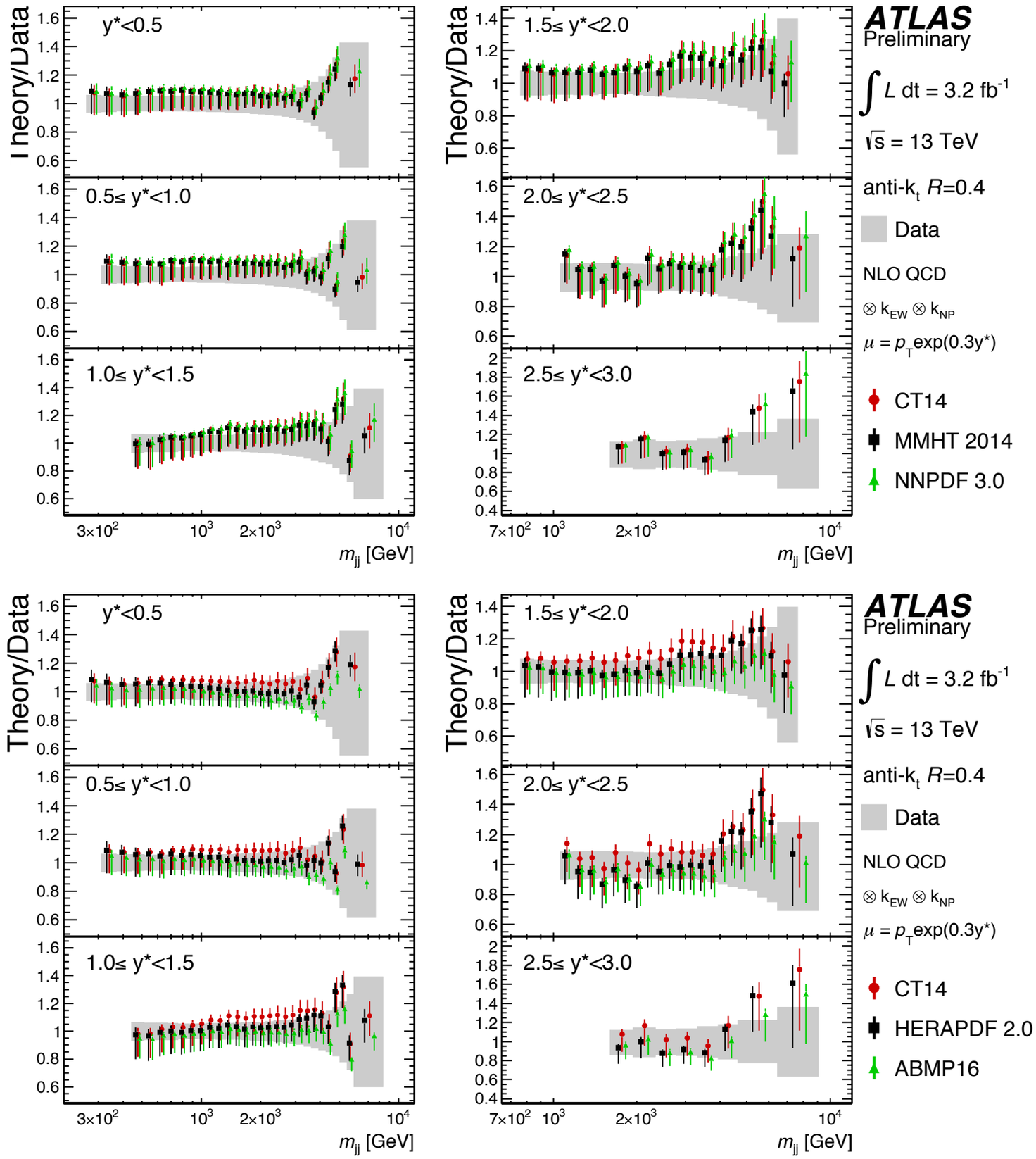

Dijet production at 13 TeV

Summary of the p-values obtained from the comparison of the dijet cross section and the NLO pQCD predictions for various PDFs and for each y^* bin.

	P_{obs}				
y^* ranges	CT14	MMHT 2014	NNPDF 3.0	HERAPDF 2.0	ABMP16
$y^* < 0.5$	79%	59%	50%	71%	71%
$0.5 \leq y^* < 1.0$	27%	23%	19%	32%	31%
$1.0 \leq y^* < 1.5$	66%	55%	48%	66%	69%
$1.5 \leq y^* < 2.0$	26%	26%	28%	9.9%	25%
$2.0 \leq y^* < 2.5$	43%	35%	31%	4.2%	21%
$2.5 \leq y^* < 3.0$	45%	46%	40%	25%	38%
all y^* bins	8.1%	5.5%	9.8%	0.1%	4.4%

$\gamma\gamma \to \ell^+\ell^-$ *at 7 TeV*

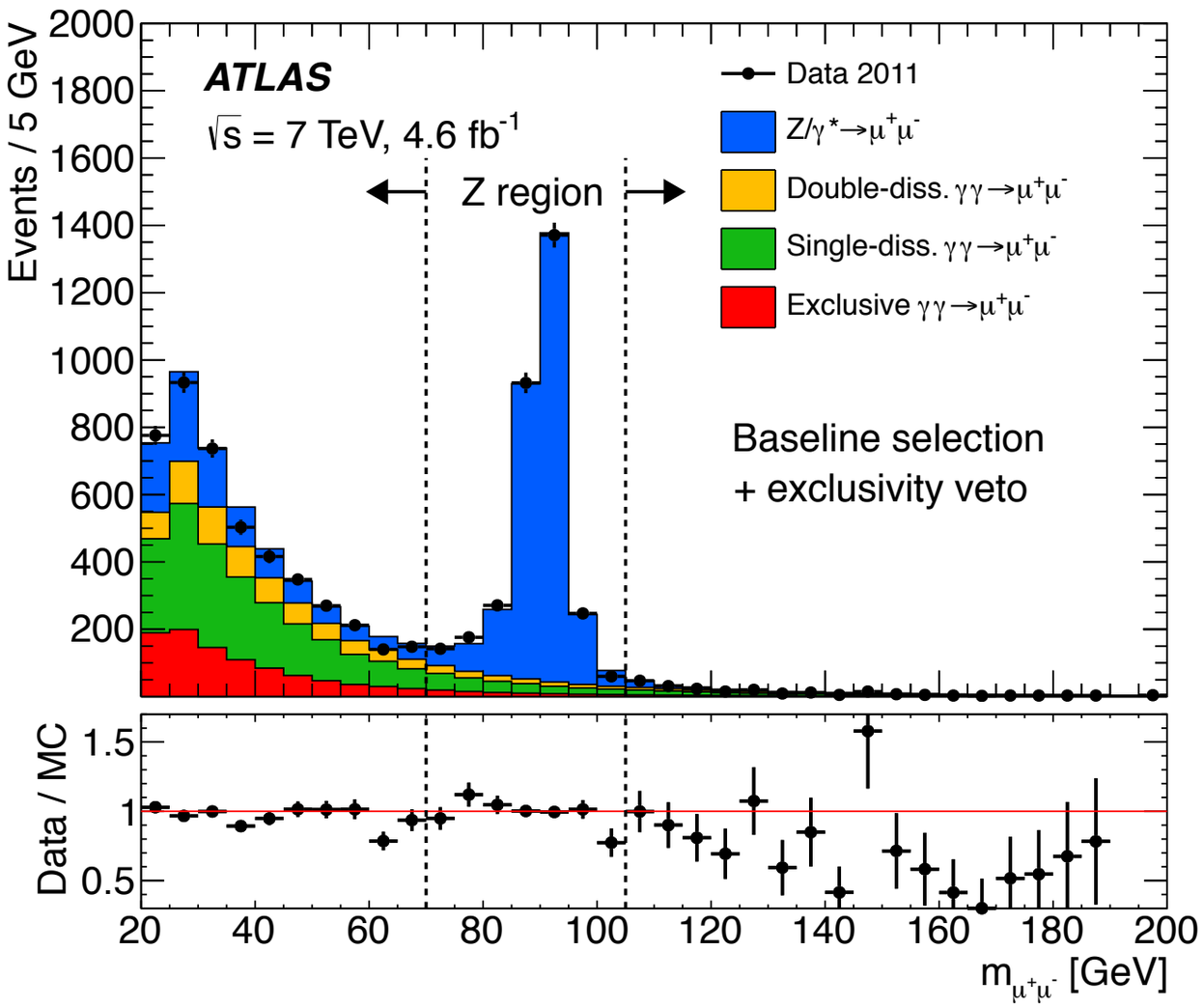

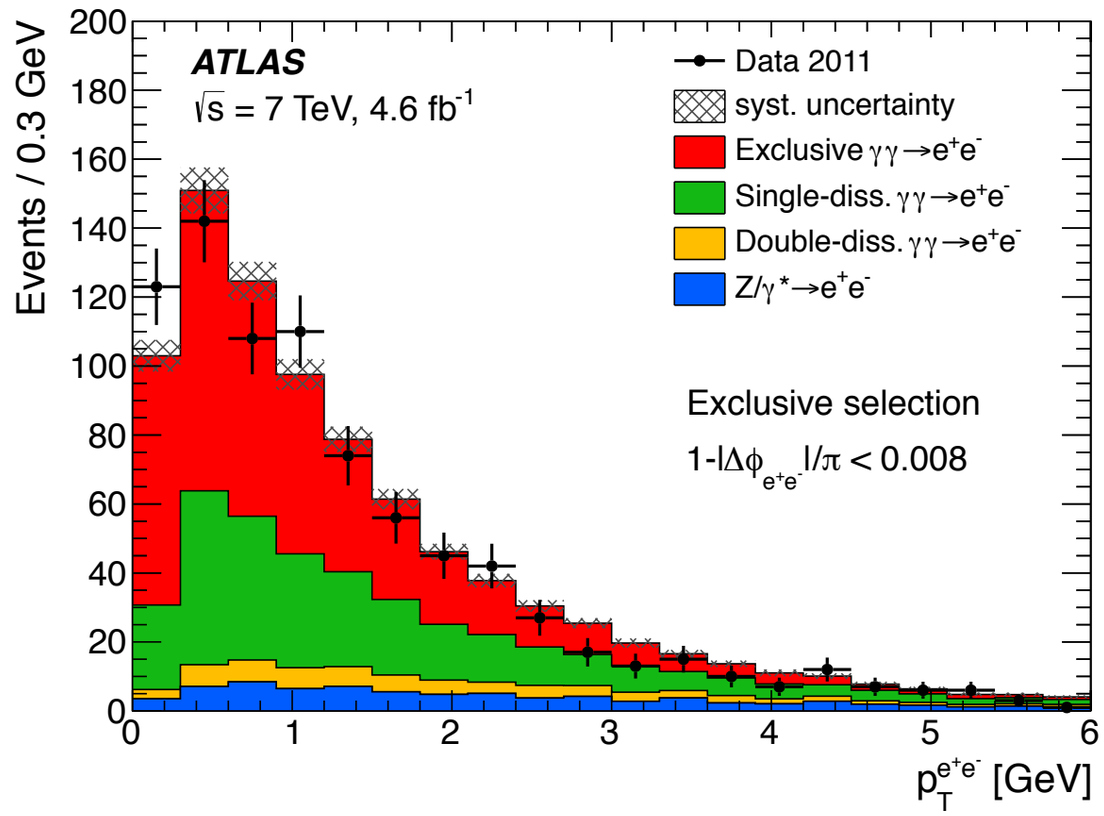

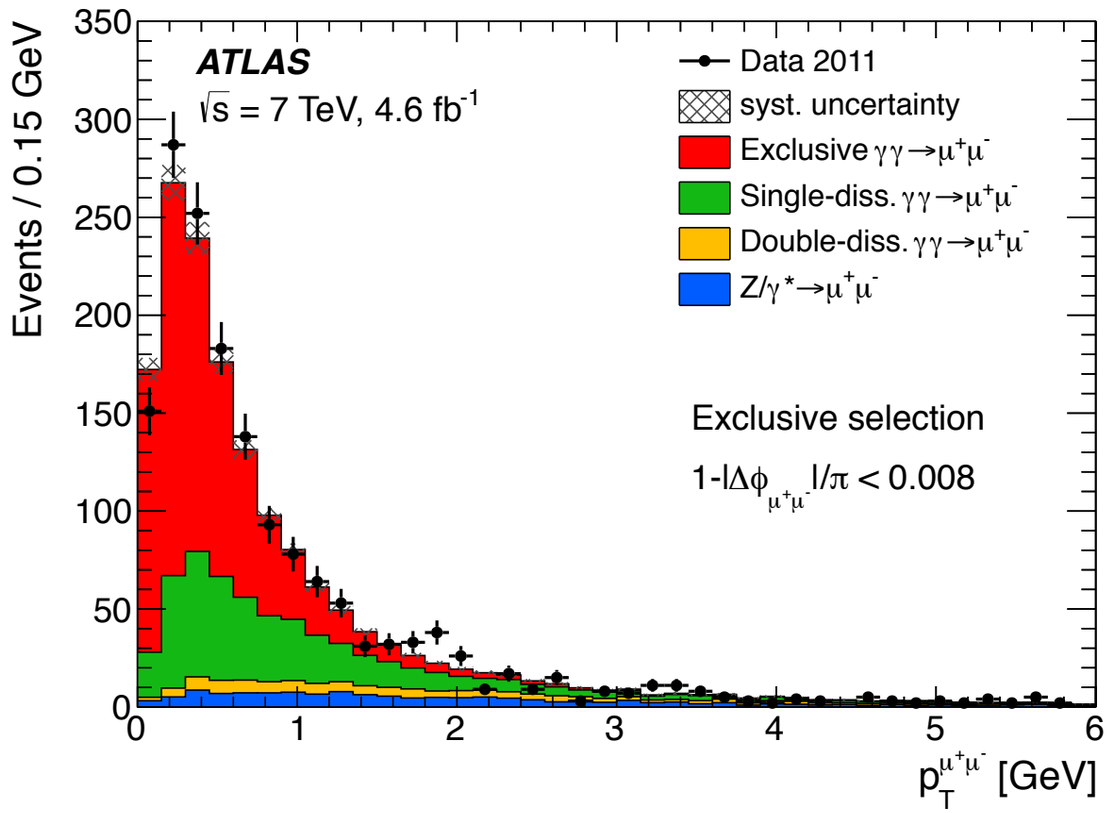

$\gamma\gamma \to \mu^+\mu^-$ *at 13 TeV*

In the Z-mass region

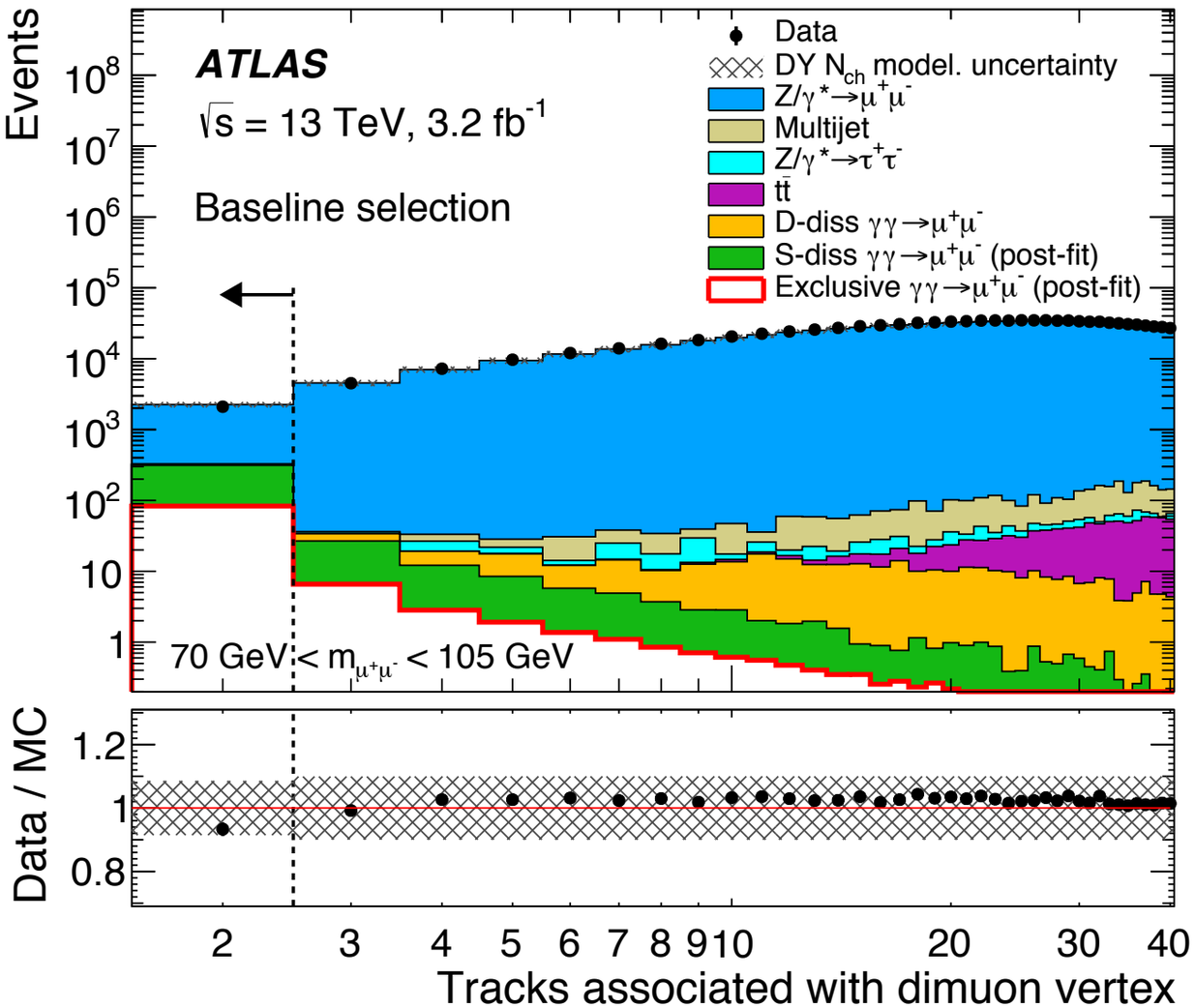

Outside the Z-mass region

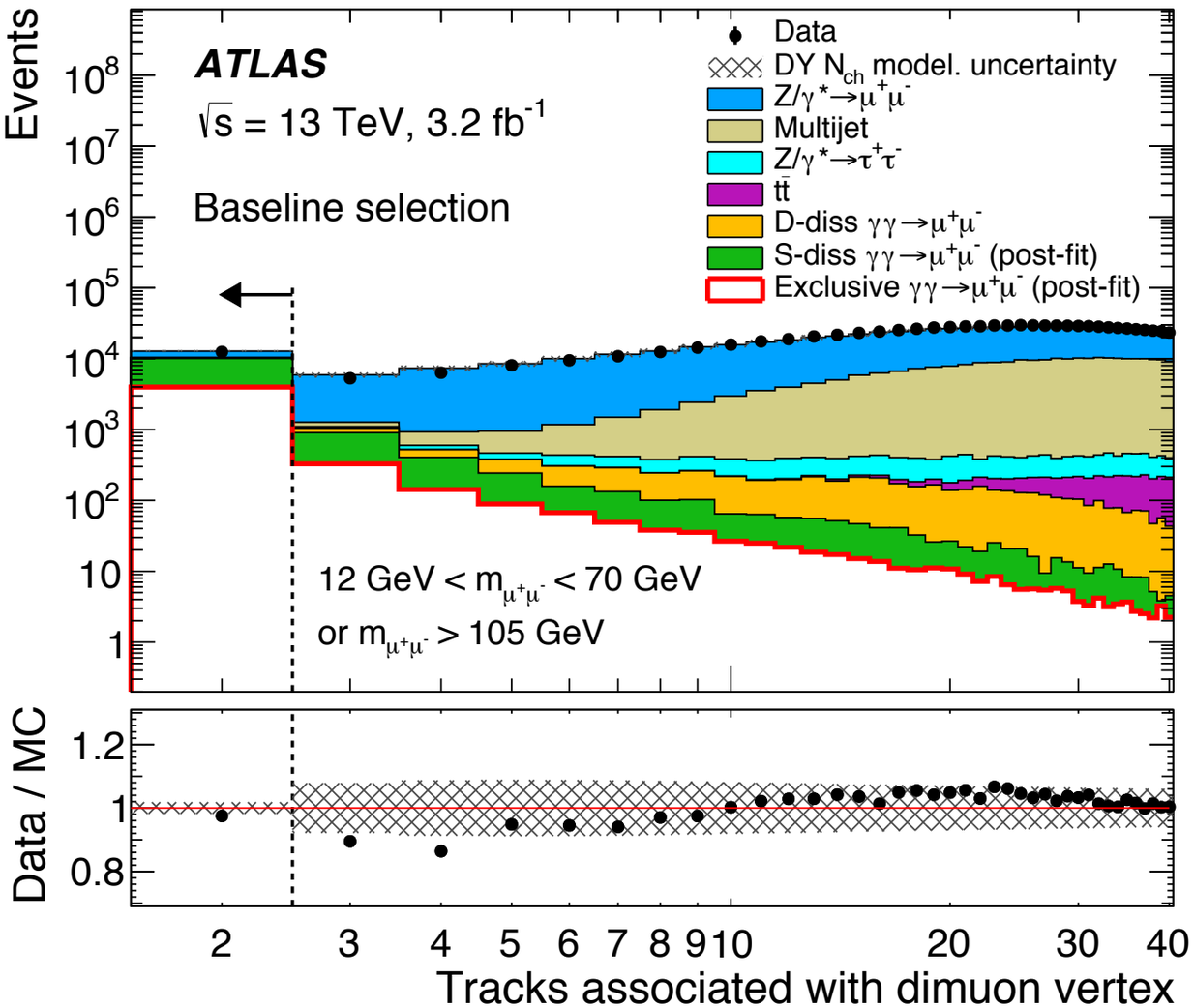

$\gamma\gamma \to W^+W^-$ at 8 TeV

	Expected Signal	Data	Total Bkg	Incl W^+W^-	Excl. $\tau\tau$	Other-VV	Other Bkg	SM/Data	ϵA (Signal)
Preselection	22.6 ± 1.9	99424	97877	11443	21.4	1385	85029	0.98	0.254
$p_{\mathrm{T}}^{\ell\ell} > 30$ GeV	17.6 ± 1.5	63329	63023	8072	4.30	896.3	54051	1.00	0.198
$\Delta z_0^{\mathrm{iso}}$ requirement	9.3 ± 1.2	23	8.3 ± 2.6	6.6 ± 2.5	1.4 ± 0.3	0.3 ± 0.2	–	0.77	0.105 ± 0.012
aQGC signal region									
$p_{\mathrm{T}}^{\ell\ell} > 120$ GeV	0.37 ± 0.04	1	0.37 ± 0.13	0.32 ± 0.12	0.05 ± 0.03	0	–	0.74	0.0042 ± 0.0005

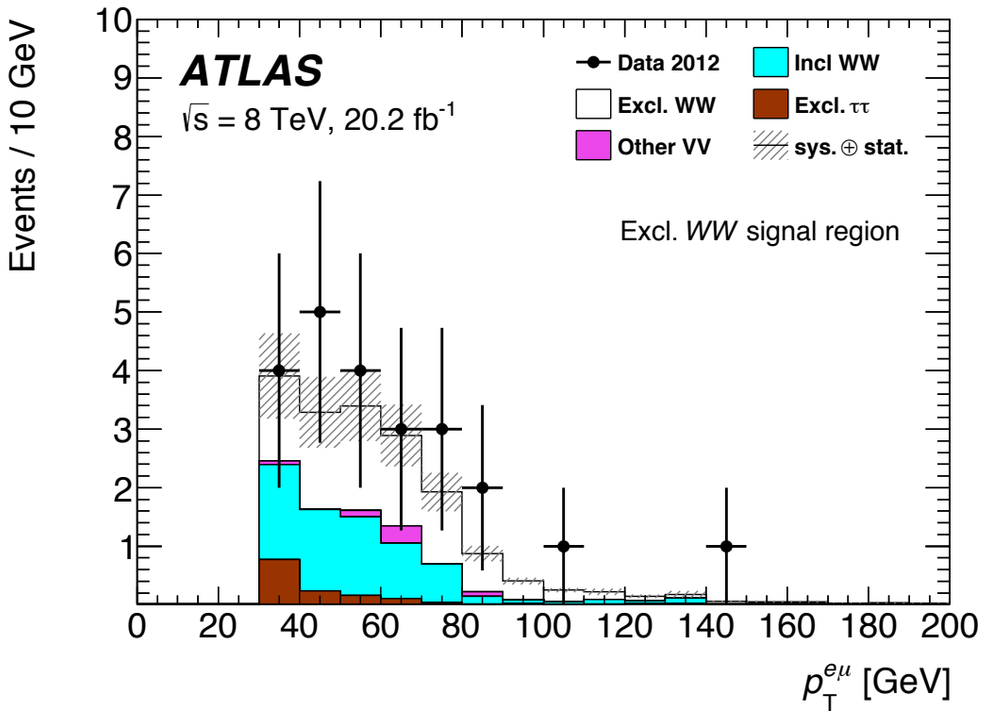

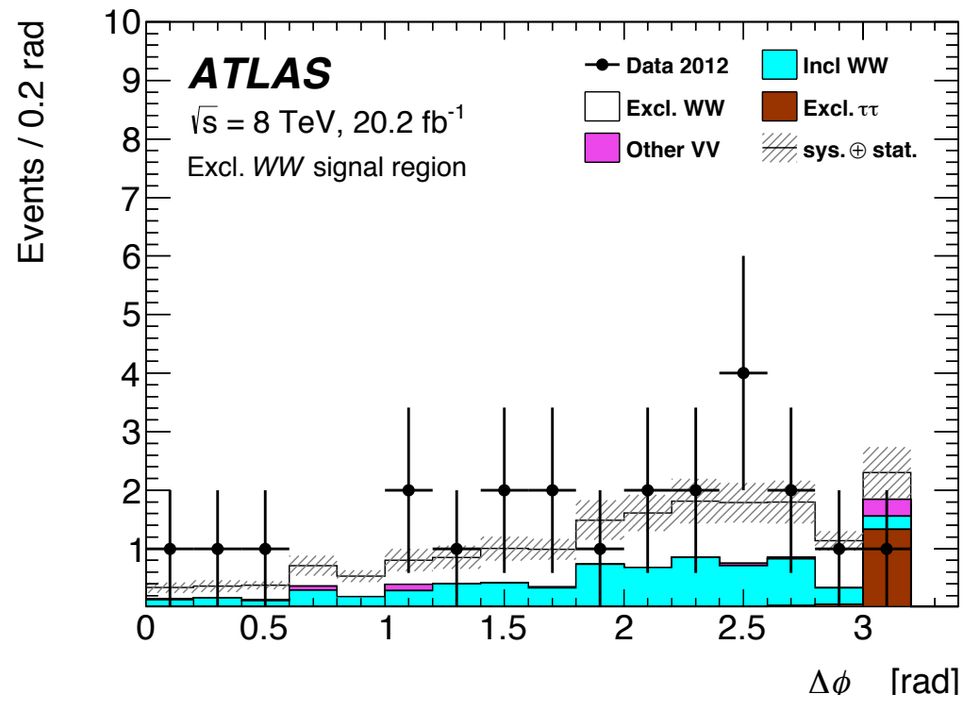

Measurement significance of 3σ. Additional cut on $\mathrm{p_T}^{e\mu}$ to enhance the aQGC contribution. Comparison with various anomalous quartic gauge coupling scenarios. New limits set.

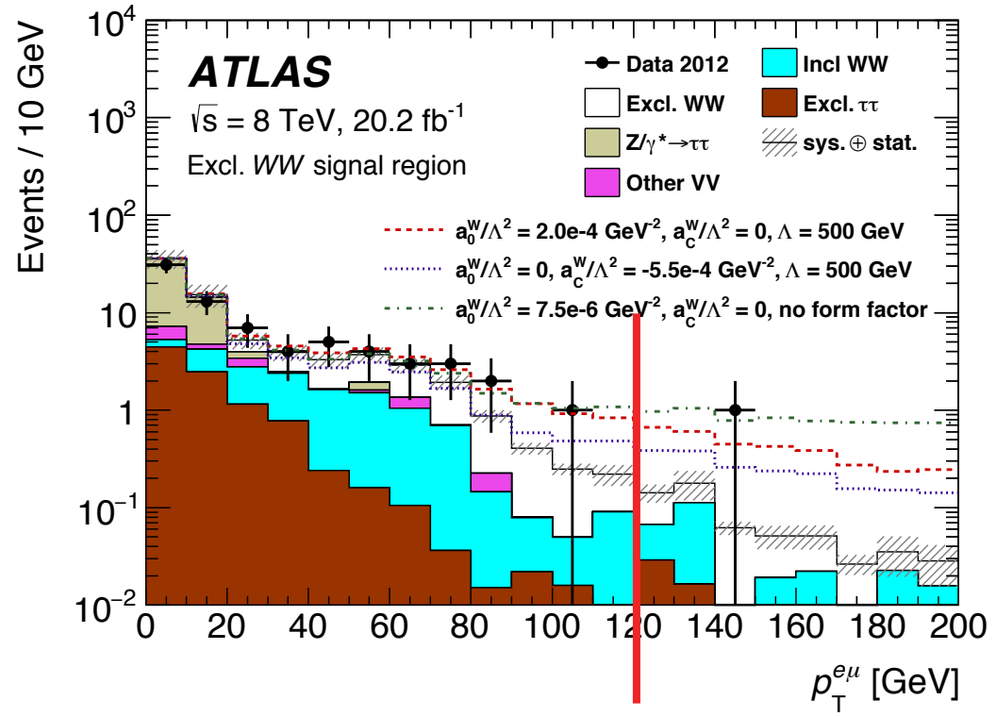

$gg \to H \to W^+W^-$ *at 8 TeV*

	Excl. H Signal	Data	Total Bkg	Incl. W^+W^-	Excl. W^+W^-	Other Bkg
Preselection	0.065 ± 0.005	129018	120090	12844	43	107200
$p_{\mathrm{T}}^{e\mu}$ >30 GeV, $m_{e\mu} < 55$ GeV, $\Delta\phi_{e\mu} < 1.8$	0.043 ± 0.004	18568	17060	2026	5.7	15030
$\Delta z_0^{\mathrm{iso}}$ requirement	0.023 ± 0.003	8	4.7 ± 1.3	1.4 ± 0.5	3.1 ± 1.3	0.2 ± 0.1
$m_{\mathrm{T}} < 140$ GeV [Signal Region]	0.023 ± 0.003	6	3.0 ± 0.8	1.0 ± 0.4	1.8 ± 0.8	0.2 ± 0.1

The predicted background from exclusive W^+W^- is derived from the observed cross section in the exclusive W pair signal region.
Reasonable agreement between data and predictions.

1.2 pb (95% CL) upper limit set on the total production cross section, while the expected limit is 0.7 pb.